Ice nucleating particles at a coastal marine boundary layer site: correlations with aerosol type and meteorological conditions

Authors: R. H. Mason[1], M. Si[1], J. Li[2], C. Chou[1], R. Dickie[1], D. Toom-Sauntry[3], C. Pöhlker[4], J. D. Yakobi-Hancock[5], L. A. Ladino[5], K. Jones[6], W. R. Leaitch[3], C. L. Schiller[6], J. P. D. Abbatt[5], J. A. Huffman[2*], A. K. Bertram[1*]

Affiliations:

[1]Department of Chemistry, University of British Columbia, Vancouver, BC, V6T1Z1, Canada

[2]Department of Chemistry and Biochemistry, University of Denver, Denver, CO, 80208, USA

[3]Climate Research Division, Environment Canada, Toronto, ON, M3H5T4, Canada

[4]Biogeochemistry Department, Max Planck Institute of Chemistry, Mainz, 55020, Germany

[5]Department of Chemistry, University of Toronto, Toronto, ON, M5S3H6, Canada

[6]Air Quality Science Unit, Environment Canada, Vancouver, BC, V6C3S5, Canada

[*]Correspondence to: bertram@chem.ubc.ca (A. K. Bertram), alex.huffman@du.edu (J. A. Huffman)

Anonymous Referee #1

Received and published: 25 June 2015

Ryan Mason 10/8/2015 4:39 PM
Comment [1]: Response to reviewers.

[A0] For clarity and visual distinction, the referee comments or questions are listed here in black and are preceded by bracketed, italicized numbers (e.g. ***[1]***). Authors' responses are offset in blue below each referee statement with matching numbers (e.g. ***[A1]***). Page and line numbers refer to online ACPD version.

Mason et al. present results on ice nucleating particles (INPs) from a coastal site in western Canada during the summer. The INP concentrations strongly correlated with fluorescent terrestrial bioparticles at high temperatures, while particles that were likely mineral dust nucleated ice at lower temperatures. However, predicted INP concentrations using different empirical parameterizations did not corroborate the observations, demonstrating the need for improved modeling of INPs. The paper is overall well written and the methods and interpretation of the results are clear. There are a few needed improvements described below, however, once these are addressed, this paper is suit- able for publication in ACP.

We thank the referee for his/her helpful comments!

General remarks:

[1] The abstract could be strengthened by adding a sentence of two of broader implications at the end. What do these results signify and how do they advance our understanding of INPs? Perhaps here, and in general throughout the manuscript, one large motivation for work such as this is that the parameterizations did not corroborate the observations, demonstrating the need for more observations to improve simulated INP concentrations and their subsequent climatic impacts.

[A1] Thank you for the suggestion. The following sentence will be added to the end of the abstract:

"This finding illustrates that additional measurements are needed to improve parameterizations of INPs and their subsequent climatic impacts. "

[2] The introduction would benefit from more background, such as on primary bioparticles versus marine bioparticles. What are some of the sources of these types? What types of bioparticles are marine? Also, the authors conclude that dust was likely observed at the lower temperatures, so some background on mineral and soil dust as IN is warranted. It would be helpful to also include previously documented temperature ranges in which each of the different types of INPs nucleate ice at (use references such as Murray et al. (2012), Conen et al. (2011), DeMott et al. (2003, 2009, 2013), O'Sullivan et al. (2014), etc.).

[A2] In the revised manuscript, we will rewrite the introduction with the referee's comments in mind.

[3] The dates of the sample collection should be provided first thing in the methods. Otherwise, there is only one figure that includes an Aug time period but the exact dates and year should be provided.

[A3] The dates of sample collection will be added to the Methods section in the revised manuscript.

[4] In the methods, the DFT measurements were conducted at, "-10 C per minute to -40 C." However, many of the results are presented in -5 C steps. Why are measurements not presented as -10, -20, -30, -40 C? Perhaps the measurements started at -15 C, but this should be explicitly stated. Were measurements acquired at -10 C? That would be an interesting comparison since the focus is on biological particles and these can nucleate ice up to -2 C.

[A4] Data was not reported at temperatures above -15 ºC since very few freezing events occurred at these warm temperatures (only 1.3 % of all droplets froze above -15 ºC). Data was not reported below -30 ºC since in some experiments all droplets froze at these temperatures, which prohibits the calculation of INP number concentrations by Eq. (1). To address the referee's comment, the following sentence will be added to Sect. 2.2.

"Here we report INP data between -15 and -30 °C as few (1.3 %) of droplets froze at temperatures > -15 C, and at temperatures < -30 C, in some experiments all droplets froze, which prohibited the calculation of INP number concentrations by Eq. (1)."

[5] Can the authors comment on the possible contribution from soil dust? Wouldn't this fluoresce as well with WIBS (as in Gabey, A.M., Stanley, W. R., Gallagher, M. W., Kaye, P.H.: The fluorescence properties of aerosol larger than 0.8 um in urban and tropical rainforest locations, Atmos. Chem. Phys., 11, 5491-5504, doi:10.5194/acp-11- 5491-2011, 2011.)?

[A5] To address the referee's comment, line 26, page 16282 will be revised to the following:

"While some non-biological species such as soot, mineral and soil dusts, polycyclic aromatic hydrocarbons, secondary organic aerosols, and humic-like substances can produce a fluorescent signal (Bones et al., 2010; Gabey et al., 2011; Lee et al., 2013; Pan et al., 1999; Pöhlker et al., 2012; Sivaprakasam et al., 2004), the number of fluorescent particles is generally considered to be a lower limit to the number of primary biological particles (Huffman et al., 2010, 2012; Pöhlker et al., 2012)."

[6] Considering the particle sizes observed and shown in Fig 6. I find it odd that these large sizes are more abundant in number than smaller particles (i.e., 0.5 to 1 um). Wouldn't the authors expect to observe smaller bioparticles, such as bacteria? Perhaps this is due to the transmission efficiency of the WIBS, which could be discussed since this is a relatively new technique.

[A6] To address the referee's comment, at the end of Sect. 2.3 we will add a discussion on the size dependent detection efficiency of the WIBS.

[7] The method for using correlation of wind speed at the site and INPs emitted from the ocean surface may not be the most direct, since the wind speed may be different over the water versus land surface. Have the authors considered estimating the wind speed from the HYSPLIT trajectories? That may lead to a better estimate of wind speeds over the ocean along the transport

paths, since most of the trajectories remained fairly low in the marine boundary layer.

[A7] To address the referee's comment, we have determining the average wind speed during each MOUDI sampling period using data collected from a height of 5 m asl by a moored buoy located approximately 35 km WSW of our sampling site (station 46206: http://ndbc.noaa.gov/station_page.php?station=46206). Little difference was found between the two wind speed measurements. Correlations using the buoy data will be added to the revised manuscript.

[8] There should be more broad discussion on the parameterizations in section 3.7. The fact that the parameterizations did not fit the observational data demonstrate the need to improve these parameterizations by conducting more observations in different locations, times of year, and land cover regimes (i.e., arid, vegetation, near BC sources such as fires, etc.).

[A8] Thank you for the suggestion. To address the referee's comment we will add the following text to the end of Sect. 3.7:

"Figure 8 suggests that additional measurements of INPs in other environments, times of year, and altitudes are needed to further test and improve current parameterizations of INPs. The results presented in Fig. 8 also indicate that the application of INP parameterizations to locations dissimilar to that of the original study used to generate the parameterizations should be done with care."

Specific comments:

[9] Page 16275, line 17: Clarify that these are chemical tracers, and if space permits, provide the tracers (i.e., MSA and Na).

[A9] This revision will be made in the final document.

[10] Page 16279, line 4: Briefly define Cfb.

[A10] For clarity, this sentence will be modified to the following in the revised manuscript:

"This region has a temperate maritime climate, characterized by warm summers, mild winters, and relatively high levels of cloud cover and precipitation. According to the Köppen-Geiger classification scheme (Kottek et al., 2006) the climate type is Cfb which denotes a mild mid-latitude and moist climate (C) with no dry season (f), and a moderate summer where the average hottest-month temperature is < 22 ºC and at least four months have an average temperature > 10 ºC (b)."

[11] Page 16280, line 4: Change "measured" to "collected".

[A11] To address the referee's comment "measured" will be changed to "determined". We feel the use of "determined" is more appropriate than "collected" since the MOUDI-DFT includes sample collection and freezing measurements.

[12] Page 16280, line 18: Spell out DFT on first occurrence.

[A12] This correction will be made.

[13] Page 16288, line 23: Instrument and sampling details for CO, NOx, and SO2 should be briefly provided in the methods.

[A13] In the revised manuscript, this information will be added to the main document.

[14] Section 3.4: Was there any correlation of INPs with wind direction?

[A14] No correlations were found between INPs and local wind direction (*R* ranged from -0.19 to -0.32). This information will be added to Sect. 3.4 to address the referee's comment.

[15] Section 3.6: In regards to the possible free tropospheric transport of dust, the authors could examine 10-day air mass back trajectories for this particular time period to evaluate the potential sources of the aerosol. For instance, if the trajectories all pass over one of the major arid regions in Asia or Africa, this would support their assumption that mineral dust contributed to the INP concentrations at -30 C.

[A15] In the revised manuscript, ten-day back trajectories will be added to the Supplement. None of the trajectories pass over major arid regions in Asia or Africa; however, this does not rule out mineral dust or soils as a source of INPs in our measurements.

[16] Page 16292, line 15: What are some of the potential sources of INP along the coastal NW that would be larger than 1 um? The vegetation coverage is discussed for the entire region in the first section of the methods, but it could be specified here what is NW of the site.

[A16] To address the referee's comment, the following will be added at the end of section 3.6:

"Vegetation NW of the sampling site closely follows that of the region, and potential sources of supermicron INPs from coastal NW include forests of coastal western hemlock."

[17] Page 16293, line 3: Up until this point, the maximum size for the WIBS used is 10 um, why the change here?

[A17] In Section 3.7 we used data from the WIBS-4A over its full size range (0.5–23.7 µm) to better match the sampling conditions used in D10 and T13, where the parameterizations were developed using total particle and fluorescent bioparticle concentrations over the full size range of the UV-APS (approximately 0.5–20 µm). This information will be added to Page 16293, line 3 for clarity.

[18] Page 16294, line 1: But in the introduction on page 16278, lines 2-3, sea salt is presented as having the ability to serve as INP. Perhaps the authors should clarify that these referenced studies investigated NaCl or sea spray to form ice at very low temperatures (roughly -35 to -58 C), thus

sea salt has the potential to form ice, yet is inefficient at temperatures relevant to heterogeneous ice nucleation.

[A18] In the revised manuscript the introduction will be modified to avoid the impression that NaCl can form ice at the temperatures we studied.

[19] Fig 2: It would be useful to, in some way, also show the trajectories colored by source group (similar colors as in Fig 3). Perhaps an additional panel with the same trajectories colored by group would suffice?

[A19] In the revised manuscript we will add an additional figure to the Supplement that will show the trajectories in Fig. 2 colored by source group.

[20] Fig 5: In the manuscript, the authors state that correlations which are insignificant ($p > 0.05$) are not discussed, yet they are shown here and are actually discussed in the manuscript. Perhaps this statement should be removed or revised if the authors choose to keep these data.

[A20] To address the referee's comment the statement "Only correlations with statistical significance (P value < 0.05) are discussed" will be changed to "In the discussion, correlations with statistical significance (P value < 0.05) are emphasized".

Anonymous Referee #2
Received and published: 31 August 2015

[A0] For clarity and visual distinction, the referee comments or questions are listed here in black and are preceded by bracketed, italicized numbers (e.g. ***[1]***). Authors' responses are offset in blue below each referee statement with matching numbers (e.g. ***[A1]***). Page and line numbers refer to online ACPD version.

In this manuscript, Mason and co-authors present an experimental study on the abundance, the nature and the origin of ice nucleating particles (INPs) measured at a coastal site in British Columbia. It was a pleasure to read this article for various reasons: it is clearly structured and well written, the applied methods are well described or cited, the measurements well documented, the data evaluation and interpretation is solid and appropriate, and the conclusions and atmospheric implications are clear and carefully formulated which I prefer versus over interpretation. In summary, this is an excellent manuscript with new and relevant results which in principle can be accepted for publication in ACP as is.

We thank the referee for his/her helpful comments!

Referee comments:
[1] I just have a few minor comments the authors may consider for the final manuscript version. My first comment refers to the mixing state of the different compounds (biological, mineral,

soot, etc.) in the aerosol size distribution. This mixing state was not measured in this study, but may have an influence on some of the conclusions, like the contributions of biological particles to the INP abundance concluded from the size distributions as shown in Figure 6. What if the larger particles are just more likely to carry a fluorescent biological particle but the ice nucleation activity is related to some other particle component? The same can happen with soot or other smaller particles that have been collected by larger particles and thus still may contribute to the ice nucleation activity of the apparently larger particles. This possibility or limitation may be mentioned somewhere in the manuscript and also in the conclusion section. This comment also refers to the need of particle mixing state information in future atmospheric INP studies. Would it e.g. be possible in future studies to co-locate the INPs with fluorescent signatures (or other particle compound or property signatures) on the same substrate?

[A1] To address the referee's comments, the following text will be added to the conclusions:

"In this paper we assumed that particles were externally mixed. In future studies it would be useful to include mixing state measurements together with studies similar to those presented here to quantify the extent of external versus internal mixing. In addition, studies that identify INPs followed by chemical composition measurements of these particles by electron microscopy (e.g. Knopf et al., 2014) or fluorescence microscopy would be useful."

[2] I agree to referee 1 that the abstract could be strengthened. I also recommend extending the conclusion section for the most important findings and atmospheric implications.

[A2] See response to Question 1 from Referee 1. In addition, the conclusion section will be extended slightly.

[3] In the abstract line 12 the correlation between INPs at -30ºC and total particles larger than 0.5 µm is mentioned. I think Figure S1 shows INP at -30ºC being equally well correlated with fluorescent and total particles. How can then be concluded for an extra contribution of non-biological particles to INPs? I recommend moving Figure S1 to the main manuscript.

[A3] At a droplet freezing temperature of -30 ºC, fluorescent bioparticles and total particles have the same linear correlation coefficient to INPs (R = 0.66). Here we are interested in the trends in R values from previous temperatures as given in Table 1 when discussing possible changes in the composition of INPs. The decrease in R from 0.83 to 0.66 between -25 and -30 ºC for fluorescent bioparticles suggests that the relative contribution of fluorescent bioparticles to the overall INP population is decreasing at temperatures below -25 ºC. On the other hand, an increase in R from 0.49 to 0.66 between -25 and -30 ºC for total particles also suggests that non-biological particles are becoming an increasingly important source of INPs at lower temperatures (given that biological particles are more poorly correlated).

We would prefer to keep Fig. S1 in the supplement since the some of the panels in Fig. S1 are the same as some of the panels in Fig. 5 in the main text. However, if the editor prefers we can move Fig. S1.

[4] The first sentence of the introduction reads as if there is no contribution of heterogeneous ice

nucleation in cirrus clouds, which certainly is not the case.

[A4] The first sentence will be rewritten to address the referee's comments.

[5] When discussion the various ice nucleation modes you may also cite Vali et al., Atmos. Chem. Phys. Discuss., 14, 22155-22162, 2014.

[A5] A reference to Vali et al. (now published in ACP) will be added to the revised manuscript.

Abstract:

Information on what aerosol particle types are the major sources of ice nucleating particles (INPs) in the atmosphere is needed for climate predictions. To determine which aerosol particles are the major sources of immersion-mode INPs at a coastal site in Western Canada, we investigated correlations between INP number concentrations and both concentrations of different atmospheric particles and meteorological conditions. We show that INP number concentrations are strongly correlated with the number concentrations of fluorescent bioparticles between -15 and -25 °C, and that the size distribution of INPs is most consistent with the size distribution of fluorescent bioparticles. We conclude that biological particles were likely the major source of ice nuclei at freezing temperatures between -15 and -25 °C at this site for the time period studied. At -30 °C, INP number concentrations are also well correlated with number concentrations of the total aerosol particles ≥ 0.5 µm, suggesting that non-biological particles may have an important contribution to the population of INPs active at this temperature. As we found that black carbon particles were unlikely to be a major source of ice nuclei during this study, these non-biological INPs may include mineral dust. Furthermore, correlations involving chemical tracers of marine aerosols and marine biological activity, sodium and methanesulfonic acid, indicate that the majority of INPs measured at the coastal site likely originated from terrestrial rather than marine sources. Finally, six existing empirical parameterizations of ice nucleation were tested to determine if they accurately predict the measured INP number concentrations. We found that none of the parameterizations selected are capable of predicting INP number concentrations with high accuracy over the entire temperature range investigated. This finding illustrates that additional measurements are needed to improve parameterizations of INPs and their subsequent climatic impacts.

Ryan Mason 10/8/2015 4:36 PM
Comment [2]: Beginning of marked-up manuscript

1. Introduction

The formation of ice in the atmosphere can occur by two primary mechanisms: homogeneous and heterogeneous ice nucleation. Homogeneous nucleation can only occur at temperatures below approximately -37 °C. However, heterogeneous nucleation can occur at all temperatures below 0 °C. In the atmosphere, heterogeneous nucleation occurs on solid or partially solid aerosol particles termed ice nucleating particles (INPs). INPs are a small subset of the total aerosol population (Rogers et al., 1998) whose unique surface properties make them capable of lowering the energy barrier to ice nucleation and hence cause freezing at warmer temperatures or lower supersaturations with respect to ice compared to homogeneous nucleation. Four modes of nucleation have been identified (Vali, 1985; Vali et al., 2015): deposition nucleation where ice forms on the INP directly from the gas phase; condensation freezing where ice forms during the condensation of water onto the INP; immersion freezing where ice forms on an INP within a supercooled droplet; and contact freezing where the impact of a supercooled droplet by an INP initiates freezing. In this study we focus on immersion freezing, which is relevant to ice formation in mixed-phase clouds.

The presence of INPs in the atmosphere can lead to changes in the microphysical properties and lifetime of clouds. As a result, a change in INP concentrations can indirectly modify climate by changing cloud optical properties, lifetime, and cloud extent (e.g. Baker, 1997; Lohmann, 2002; Storelvmo et al., 2011; Creamean et al., 2013). Currently, the role of INPs in climate change is highly uncertain (Boucher et al., 2013). To predict the role of INPs in climate change and precipitation, information on what particle types are the major sources of INPs in the atmosphere is needed. Possible candidates for INPs in the atmosphere include mineral dust, primary biological particles, and black carbon (BC). Primary biological INPs are

Ryan Mason 10/4/2015 10:22 AM
Deleted: At temperatures below approximately -37 °C ice nucleation of solution droplets in the atmosphere occurs by a homogeneous process, but at warmer temperatures ice can also form by heterogeneous nucleation on solid or partially solid aerosol particles called ice nucleating particles (INPs).

368 believed to be dominant above -15 °C while below this temperature non-biological INPs may be
369 of greater importance (Murray et al., 2012).

370 Mineral dust particles have long been known to be efficient INPs (Mason and Maybank,
371 1958). Numerous laboratory studies have found that different types of mineral dust particles can
372 effectively nucleate ice in both the immersion and deposition modes; for example kaolinite
373 (Lüönd et al., 2010; Wheeler and Bertram, 2012), Arizona test dust (Kanji and Abbatt, 2010;
374 Knopf and Koop, 2006; Marcolli et al., 2007; Niedermeier et al., 2010), NX illite (Broadley et
375 al., 2012), natural Asian and Saharan dust samples (Field et al., 2006; Kulkarni, 2010), and more
376 recently feldspar (Atkinson et al., 2013; Yakobi-Hancock et al., 2013). Both field studies
377 (DeMott et al., 2003; Cziczo et al., 2004; Richardson et al., 2007; Klein et al., 2010; Chou et al.,
378 2011; Creamean et al., 2013) and modeling studies (Hoose et al., 2010b) also suggest that
379 mineral dust can be a dominant INP in the atmosphere.

380 Primary biological particles have also been identified as a possible source of INPs (e.g.
381 Szyrmer and Zawadzki, 1997; Möhler et al., 2007; Garcia et al., 2012; Hiranuma et al., 2015).
382 The ocean and continents are both potential sources of ice-active primary biological particles
383 (Hoose and Möhler, 2012; Murray et al., 2012). Model studies have shown that biological
384 particles may not be important for ice nucleation on a global and annual scale (Hoose et al.,
385 2010; Sesartic et al., 2013; Spracklen and Heald, 2014), but may be important on regional and
386 seasonal scales, especially if concentrations of biological particles are high or concentrations of
387 other types of INPs are low (Phillips et al., 2009; Sun et al., 2012; Burrows et al., 2013;
388 Creamean et al., 2013; Yun and Penner, 2013; Costa et al., 2014; Spracklen and Heald, 2014).

389 Ice-active biological particles from continental sources include bacteria (e.g. Maki et al.,
390 1974; Lindow et al., 1978; Maki and Willoughby, 1978; Kozloff et al., 1983), fungal spores (e.g.

Ryan Mason 10/4/2015 10:23 AM
Deleted: Particle types that we focused on as possible candidates for INPs included primary biological particles, black carbon (BC), and primary marine particles.

Ryan Mason 10/4/2015 10:29 AM
Moved down [1]: Biological particles found to efficiently nucleate ice include bacteria (e.g. Maki et al., 1974; Lindow et al., 1978; Maki and Willoughby, 1978; Kozloff et al., 1983), fungi (e.g. Jayaweera and Flanagan, 1982; Tsumuki et al., 1992; Richard et al., 1996; Iannone et al., 2011; Haga et al., 2013; Morris et al., 2013), and pollen (e.g. Diehl et al., 2001, 2002; von Blohn et al., 2005; Pummer et al., 2012; Augustin et al., 2013; Hader et al., 2014; O Sullivan et al., 2015). Strong correlations between number concentrations of INPs and primary biological particles have been found during field studies (Prenni et al., 2009b, 2013; Huffman et al., 2013; Tobo et al., 2013), and biological particles have been observed in ice-crystal residuals of mixed-phase clouds (e.g. Pratt et al., 2009), cloud water (e.g. Joly et al., 2014), and snow samples (e.g. Christner et al., 2008; Morris et al., 2008; Hill et al., 2014). Ice-active biological particles have also been associated with soils (Conen et al., 2011; O'Sullivan et al., 2014; Tobo et al., 2014; Fröhlich-Nowoisky et al., 2015).

Ryan Mason 10/4/2015 10:29 AM
Moved (insertion) [1]

Ryan Mason 10/4/2015 10:30 AM
Deleted: Biological particles found to efficiently nucleate ice

Jayaweera and Flanagan, 1982; Tsumuki et al., 1992; Richard et al., 1996; Iannone et al., 2011; Haga et al., 2013; Morris et al., 2013), and pollen (e.g. Diehl et al., 2001, 2002; von Blohn et al., 2005; Pummer et al., 2012; Augustin et al., 2013; Hader et al., 2014; O Sullivan et al., 2015). In addition, strong correlations between number concentrations of INPs and primary biological particles have been found during studies in the Amazon and United States in forested regions (Prenni et al., 2009b, 2013; Huffman et al., 2013; Tobo et al., 2013), and biological particles have been observed in ice-crystal residuals of mixed-phase clouds (e.g. Pratt et al., 2009), cloud water (e.g. Joly et al., 2014), and snow samples (e.g. Christner et al., 2008; Morris et al., 2008; Hill et al., 2014). Ice-active biological particles have also been associated with soils (Conen et al., 2011; O'Sullivan et al., 2014; Tobo et al., 2014; Fröhlich-Nowoisky et al., 2015).

Biological material found in the ocean that may be a source of INP in the atmosphere includephytoplankton, bacteria, and biological material in the sea surface microlayer. Studies have indicated bacteria and phytoplankton found in seawater and sea ice are a potential source of INP in the atmosphere (Schnell, 1975, 1977; Schnell and Vali, 1975; Jayaweera and Flanagan, 1982; Parker et al., 1985; Alpert et al., 2011; Knopf et al., 2011). Material in the sea surface microlayer has also been found to exhibit ice-activity (Wilson et al., 2015), and previous work has indicated that biological material generated during phytoplankton blooms may be a source of INPs in the atmosphere (Prather et al., 2013; DeMott et al., 2015). The modeling work of Burrows et al. (2013) indicates that ice-active primary biological particles from the ocean may be particularly important in remote regions such as the Southern Ocean.

Another potential type of INP in the atmosphere is BC (Kärcher et al., 2007). Laboratory studies have given varying results on whether BC particles act as efficient INPs under atmospherically-relevant conditions (e.g. Gorbunov et al., 2001; Möhler et al., 2005; Dymarska

Ryan Mason 10/4/2015 10:30 AM
Deleted: S

Ryan Mason 10/4/2015 10:30 AM
Deleted: field studies

Ryan Mason 10/4/2015 10:33 AM
Deleted: source

et al., 2006; Kärcher et al., 2007; DeMott et al., 2009; Friedman et al., 2011; Cziczo et al., 2013; Brooks et al., 2014), although BC is generally considered to be less efficient than mineral dust in the immersion mode (Hoose and Möhler, 2012; Murray et al., 2012; and references therein). Field studies have also produced varying results (e.g. Lin et al., 2006; Cozic et al., 2008; Kamphus et al., 2010; Twohy et al., 2010; Ebert et al., 2011; Corbin et al., 2012; Cziczo et al., 2013; Knopf et al., 2014; McCluskey et al., 2014). Models have suggested that carbonaceous aerosols may have a significant indirect effect on climate if they efficiently nucleate ice (e.g. Lohmann, 2002; Liu et al., 2009; Penner et al., 2009; Yun and Penner, 2013).

To determine which aerosol particles are the major source of INPs in the immersion mode at a coastal site in Western Canada, we investigate correlations between INP number concentrations and both concentrations of different atmospheric particle types and meteorological conditions. Measurements were conducted in August 2013 as part of the NETwork on Climate and Aerosols: addressing key uncertainties in Remote Canadian Environments (NETCARE) project (http://netcare-project.ca/). A primary goal of the study was to investigate whether primary biological particles and BC particles are a major source of INPs at this site and determine if the ocean contributes to the measured INP population at this coastal site. In addition, we also test the ability of parameterizations reported in the literature at predicting the INP number concentrations measured at this coastal site.

2. Methods

2.1 Site description and instrument location

Measurements were performed at Amphitrite Point (48.92° N, 125.54° W) on the west coast of Vancouver Island in British Columbia, Canada. This was also the location of studies on ozone (McKendry et al., 2014) and cloud condensation nuclei (Yakobi-Hancock et al., 2014).

Ryan Mason 10/4/2015 10:34 AM
Deleted: Ambient measurements have found INPs in air masses above oceans and coastal sites (e.g. Bigg, 1973; Schnell, 1977; Flyger and Heidam, 1978; Saxena, 1983; Rosinski et al., 1995; Rogers et al., 2001; Prenni et al., 2009a), with some of the INPs identified as biological (e.g. Jayaweera and Flanagan, 1982). Studies have also indicated the potential of marine particles as a source of ice nuclei, including bacteria and phytoplankton found in seawater and sea ice (Schnell, 1975, 1977; Schnell and Vali, 1975; Parker et al., 1985; Knopf et al., 2011; Alpert et al., 2011), synthetic sea-salt or sodium chloride particles (Wise et al., 2012; Wagner and Möhler, 2013; Schill and Tolbert, 2014), generated sea spray aerosol using ocean water (DeMott et al., 2013; Prather et al., 2013), and material in the sea surface microlayer (Wilson et al., 2015). It is therefore possible that the release of biological particles from the oceans may be a source of INPs in the atmosphere. The modeling work of Burrows et al. (2013) indicates that marine INPs may be particularly important in remote regions such as the Southern Ocean.

Ryan Mason 10/4/2015 10:37 AM
Deleted: ,

Ryan Mason 10/4/2015 10:37 AM
Deleted: ,

Ryan Mason 10/4/2015 10:37 AM
Deleted: or primary marine particles are a major source of INPs at this coastal site

Amphitrite Point (Fig. 1) is located approximately 2.2 km south of the town of Ucluelet (population of 1627 in 2011; Statistics Canada, 2012). The largest nearby population centers are Nanaimo 120 km to the east, Victoria 170 km to the southeast, and Vancouver 180 km to the east. This region has a temperate maritime climate, characterized by warm summers, mild winters, and relatively high levels of cloud cover and precipitation. According to the Köppen-Geiger classification scheme (Kottek et al., 2006), the climate type is Cfb which denotes a mild mid-latitude and moist climate (C) with no dry season (f), and a moderate summer where the average hottest-month temperature is < 22 ºC and at least four months have an average temperature > 10 ºC (b). Local forests contain predominantly coniferous tree species including western hemlock, western redcedar, and Douglas-fir that is characteristic of most low-elevation sites along the west coast of Canada (Austin et al., 2008). The Pacific Ocean is west and south of the site, where the mixing of iron-rich coastal waters with nitrate-rich oceanic waters produces a zone of high primary productivity (Whitney et al., 2005; Ribalet et al., 2010). Measurements were carried out from August 6–27, 2013. Specifics on the sampling times (i.e. start and end times) are given in Table S1 of the Supplement.

Ryan Mason 10/4/2015 10:40 AM
Deleted: , falling under the Cfb climate type of the Köppen-Geiger classification scheme (Kottek et al., 2006)

Aerosol instrumentation was located in one of two mobile laboratories; one specific to the NETCARE project (labeled 1 in Fig. 1) and one operated by Environment Canada, the British Columbia Ministry of Environment, and Metro Vancouver (labeled 2 in Fig. 1). Aerosols were sampled through louvered total suspended particulate inlets (Mesa Labs Inc., Butler, NJ, USA) or louvered PM_{10} inlets (Thermo Scientific, Waltham, MA, USA) atop masts extending 5.5 m agl. The two mobile laboratories were approximately 20 m above mean sea level and 100 m from the high tide line of the Pacific Ocean (McKendry et al., 2014). A row of trees and shrubs approximately 2–10 m in height stood between the laboratories and the rocky shoreline.

Adjacent to the laboratories on their seaward side was Amphitrite Lighthouse (labeled 3 in Fig. 1) and Wild Pacific Trail, local tourist attractions and a source of foot traffic during fair weather. Immediately north and east of the site was a station of the Canadian Coast Guard (labeled 4 in Fig. 1).

The majority of the meteorological parameters reported in this study were measured at Amphitrite Lighthouse, located approximately halfway between the mobile laboratories and the ocean. Relative humidity and temperature were monitored using an HMP45C probe (Campbell Scientific, Logan, UT, USA) with accuracies of ± 3 % and ± 0.2 °C, respectively. Wind direction and wind speed were determined by a model 05305L Wind Monitor (R. M. Young, Traverse City, Michigan, USA) to a respective accuracy of ± 3° and ± 0.2 m s^{-1}. Measurements of wind speed were also obtained from a moored buoy located in La Perouse Bank, approximately 35 km to the WSW of the Amphitrite Point sampling site (station 46206; 48.84° N, 126.00 °W; National Data Buoy Center, 2013). The cup anemometer used to measure wind speed on the buoy was positioned at 5 m asl.

2.2 Ice nucleating particle measurements

INP number concentrations in the immersion mode were determined using the micro-orifice uniform deposit impactor-droplet freezing technique (MOUDI-DFT; Mason et al., 2015). A Model II 120R MOUDI (MSP Corp., Shoreview, MN, USA) collected size-fractionated aerosol samples by inertial separation (Marple et al., 1991) onto hydrophobic glass cover slips (HR3-215; Hampton Research, Aliso Viejo, CA, USA). To compensate for the thickness of the hydrophobic glass cover slips, spacers were placed between the MOUDI stages. Custom substrate holders were added to the MOUDI impaction plates to maintain consistent positioning of the hydrophobic glass cover slips within the impactor (Mason et al., 2015). Samples from

MOUDI stages 2–8 were used in this study, corresponding to a particle size range of 10–0.18 µm (50 % cutoff aerodynamic diameter). Thirty-four sets of MOUDI samples were collected; 18 during the day and 16 at night. The average collection time of a MOUDI sample was 7.8 hours. Details of each INP sampling period are available in Table S1 of the Supplement.

The ice-nucleating ability of particles collected by the MOUDI was then determined by the droplet freezing technique (DFT; Koop et al., 2000; Iannone et al., 2011; Mason et al., 2015; Wheeler et al., 2015). Within 24 hours of collection, samples were placed in a temperature- and humidity-controlled flow cell that was coupled to an optical microscope (Axiolab; Zeiss, Oberkochen, Germany) with a 5× magnification objective. At a sample temperature of 0 °C a humidified gas flow was introduced, resulting in the formation of water droplets on the sample. Following droplet growth by condensation and coalescence, the droplet size was decreased with a dry gas flow to a final size of approximately 80–160 µm in diameter. On average, more than 99 % of particles on the surface of the hydrophobic glass cover slip were incorporated into droplets by this procedure. Closing valves upstream and downstream of the cell then isolated the flow cell, and the sample temperature was lowered at a constant rate of -10 °C min^{-1} to -40 °C. This cooling rate was chosen to minimize the freezing of a liquid droplet by contact with a growing ice crystal. Recent work suggests that changing the cooling rate by an order of magnitude may lead to a shift in freezing temperatures of approximately 0.5–2 °C (Murray et al., 2011; Broadley et al., 2012; Welti et al., 2012; Wright and Petters, 2013; Wright et al., 2013; Wheeler et al., 2015). During droplet growth, evaporation, and cooling, a CCD camera connected to the optical microscope recorded a digital video of the sample. Using the video timestamp and a resistance temperature detector positioned within the flow cell, which was calibrated against the melting point of water droplets approximately 100 µm in diameter, the freezing temperature of each

Ryan Mason 10/4/2015 10:42 AM
Deleted: DFT

574 droplet was found by manually noting the increase in droplet opacity immediately following ice
575 nucleation.

576 Since a small fraction of the sampled particles (less than 1 % on average) was not
577 included in the droplets, there was the possibility of deposition nucleation as well. However,
578 based on an analysis of the videos recorded during the ice nucleation experiments, fewer than 3
579 % of all freezing events observed were the result of deposition nucleation. Due to the low
580 occurrence of deposition nucleation, only immersion freezing results are reported.

581 The atmospheric number concentration of INPs within the size cut of each MOUDI stage,
582 [INPs(T)], was evaluated using the following equation:

583 $$[\mathrm{INPs}(T)] = -\ln\left(\frac{N_u(T)}{N_o}\right) N_o \left(\frac{A_{\mathrm{deposit}}}{A_{\mathrm{DFT}} V}\right) f_{nu} f_{ne} \quad (1)$$

584 where $N_u(T)$ is the number of unfrozen droplets at temperature T, N_o is the total number of
585 droplets, $A_{deposit}$ is the total area of the sample deposit on the hydrophobic glass cover slips, A_{DFT}
586 is the area of the sample analyzed by the DFT, V is the volume of air sampled by the MOUDI, f_{nu}
587 is a correction factor to account for changes in particle concentration across each MOUDI
588 sample (because the DFT analyzes only a fraction of the entire sample), and f_{ne} is a correction
589 factor to account for the uncertainty associated with the number of nucleation events in each
590 experiment following Koop et al. (1997). Additional details are available in Mason et al. (2015).
591 Equation (1) takes into account the possibility of multiple INPs being contained in a single
592 droplet using the method of Vali (1971). The total INP number concentration was found by
593 summing the INP number concentrations over all analyzed MOUDI stages. Here we report INP
594 data between -15 and -30 °C as few (1.3 %) of droplets froze at temperatures > -15 °C, and in
595 some experiments all droplets were frozen at temperatures < -30 °C, which prohibited the

596 calculation of INP number concentrations by Eq. (1). INP number concentrations have been
597 adjusted to standard temperature and pressure.

598 **2.3 Total and fluorescent aerosol measurements with sizes ≥ 0.5 μm**

599 A model-4A waveband integrated bioaerosol sensor (WIBS-4A; Droplet Measurement
600 Technologies, Boulder, CO, USA) was used to find both the total and fluorescent aerosol number
601 concentrations with sizes ≥ 0.5 μm. Particles that enter the WIBS-4A first transect a continuous-
602 wave 635 nm diode laser. The forward-scattered light from the continuous-wave laser is detected
603 with a quadrant photomultiplier tube for the determination of particle size and asymmetry factor
604 based on the signal intensity and asymmetry, respectively. The detected forward-scattered light
605 also triggers excitation pulses from xenon lamps, the first at a wavelength of 280 nm and the
606 second at 370 nm. The excitation pulses may lead to fluorescent emission from the particle,
607 which is then collected in two wavelength ranges: 310–400 nm (short wavelength region) and
608 420–650 nm (long wavelength region). This results in sample information provided for each
609 particle in three fluorescence channels: excitation at 280 nm, emission in the short wavelength
610 region (FL1); excitation at 280 nm, emission in the long wavelength region (FL2); and excitation
611 at 370 nm, emission in the long wavelength region (FL3). Detailed descriptions of the instrument
612 can be found in Kaye et al. (2005), Gabey et al. (2010), and Healy et al. (2012a). The sample and
613 total flow rates of the WIBS-4A were 0.63 and 2.3 L min^{-1}, respectively, and number
614 concentrations have been adjusted to standard temperature and pressure.

615 The fluorescent channels used in the WIBS-4A allow for the detection of fluorophores
616 characteristic of biological activity. These fluorophores include the amino acid tryptophan, the
617 cofactor NAD(P)H, and the micronutrient riboflavin. While some non-biological species such as
618 soot, mineral dusts, polycyclic aromatic hydrocarbons, secondary organic aerosols, and humic-

like substances can produce a fluorescent signal (Pan et al., 1999; Sivaprakasam et al., 2004; Bones et al., 2010; Gabey et al., 2011; Pöhlker et al., 2012; Lee et al., 2013), the number of fluorescent particles is generally considered to be a lower limit to the number of primary biological particles (Huffman et al., 2010, 2012; Pöhlker et al., 2012). In addition, fluorescence microscopy measurements of samples collected during this field study show high concentrations of fluorescent biological particles (see below). Therefore, fluorescent particles detected using the WIBS-4A are hereafter referred to as fluorescent bioparticles.

Although the WIBS was used to determine the total and fluorescent aerosol number concentrations with sizes ≥ 0.5 µm, it should be noted that the counting efficiency of the WIBS for polystyrene latex spheres with particle diameters of 0.5 µm is roughly 50 % (Healy et al., 2012b). Hence, concentration of particles reported here in the 0.5–1 µm size range should be considered as lower limits.

2.4 Fluorescence microscopy

Aerosol samples were collected onto glass cover slips using a custom single-stage impactor operating at a flow rate of 1.2 L min^{-1} with a 50 % cutoff aerodynamic diameter of 0.5 µm. Prior to sample collection, the substrates were coated with a thin layer of high viscosity grease (Baysilone grease, Bayer, Germany) to reduce particle bounce.

Fluorescence microscopy images were taken on a BZ-9000 fluorescence microscope (Keyence, Inc., Osaka, Japan) equipped with a 120 W super high-compression mercury lamp and a 1.5 megapixel monochrome CCD camera. Images were obtained using the following fluorescence filters: OP-66834 DAPI-BP (λ_{ex} = 360/20 nm, $\lambda_{dichroic}$ = 400 nm, λ_{abs} = 460/25 nm), OP-66836 GFP-BP (λ_{ex} = 470/20 nm, $\lambda_{dichroic}$ = 495 nm, λ_{abs} = 535/25 nm), and OP-66838 TexasRed (λ_{ex} = 560/20 nm, $\lambda_{dichroic}$ = 595 nm, λ_{abs} = 630/30 nm). Filter specifications are given

as wavelength of maximum absorbance or excitation and full width at half maximum (λ/FWHM).

2.5 Black carbon (BC) measurements

BC mass concentrations were measured using a multi-angle absorption photometer (MAAP model 5012; Thermo Scientific, Franklin, MA, USA). Detailed descriptions of the MAAP are available in Petzold et al. (2002), Petzold and Schönlinner (2004), and Petzold et al. (2005). Within the MAAP, particles are continuously collected on a glass fiber filter. The intensity of transmitted and forward-scattered light through the aerosol particle layer and filter matrix is measured by a photodetector located beneath the filter at a frequency of 1 Hz. The signal strength is attenuated by the presence of both light-absorbing particles and particles that cause backscattering. As the angular distribution of back-scattered light is related to the fraction of non-absorbing particles (Petzold and Schönlinner, 2004), four additional photodetectors located above the filter are used to quantify the non-absorbing component of the sample. The absorbance by the collected aerosol is then related to a mass of BC using a mass-specific absorption coefficient of 6.6 $m^2 g^{-1}$. Mass concentrations have been adjusted to standard temperature and pressure.

Non-BC material such as mineral dusts and brown carbon can also absorb 670 nm wavelength light used in the MAAP, albeit with smaller absorption coefficients than BC (Yang et al., 2009). We follow the recommendation of Petzold et al. (2013) for BC data derived from optical absorption methods and hereafter refer to MAAP data as measurements of equivalent black carbon (eBC).

2.6 Tracers of anthropogenic aerosols

Measurements of CO, NO_x, and SO_2 were used to identify anthropogenic contributions to the sampled air masses as sources of these gases include fossil fuel combustion and biomass burning (Galanter et al., 2000; Gadi et al., 2003; United States Environmental Protection Agency, 2014). CO concentrations were monitored using a Thermo Fisher Scientific 48i-TL, an absorbance-based analyzer using infrared light at a wavelength of 4.6 µm. NO_x concentrations were monitored using chemiluminescence with a Thermo Fisher Scientific 42i. This instrument first converts NO_2 to NO, which then reacts with ozone to produce luminescence of intensity in proportion to the level of NO_x. A Teledyne API T100U, using fluorescence emitted by SO_2 under excitation by ultraviolet light, monitored SO_2 concentrations. Data were collected for each instrument at a frequency of 1 min^{-1}.

2.7 Ion measurements

Ryan Mason 10/4/2015 10:46 AM
Deleted: 6

Size-resolved aerosol samples were collected on Teflon® filters (Pall Corporation, Port Washington, NY, USA) using a second MOUDI (model 110R). Samples were collected on the inlet, stage 1, and stages 7–10 of the MOUDI with stages 2–6 being removed prior to collection. The flow rate through the MOUDI was on average 24 L min^{-1}, resulting in a collected size range of 0.068 µm to > 20 µm (50 % cutoff aerodynamic diameter). Collection times ranged from approximately 45–49 hours and samples were stored at 4 °C for a period of one month before analysis.

Mass concentrations of sodium and methanesulfonic acid (MSA) were found using cationic and anionic chromatography following the method of Phinney et al. (2006). Briefly, filters were extracted with sonication in 10 mL of deionized water for 1 hour, and samples were analyzed with a Dionex DX600 ion chromatograph using an AS11-HC column and a CS12 column for anions and cations, respectively. Filter blanks were measured to be below the limit of

detection for both analytes. Mass concentrations were adjusted to standard temperature and pressure.

2.8 Back trajectories

Ryan Mason 10/4/2015 10:46 AM
Deleted: 7

Back trajectories spanning a period of 72 hours were calculated for each sampling period using the Hybrid Single-Particle Lagrangian Integrated Trajectory (HYSPLIT4) model of the National Oceanographic and Atmospheric Administration and the GDAS1 meteorological data archive (Draxler and Rolph, 2014). To determine if the air mass changed during a sampling period, back trajectories were initiated at the beginning of the sampling period and every 2 hours until the end of the sampling period. Back trajectories were used to assign each sampling period to one of four general air mass categories: (i) *coastal NW* where boundary layer air (defined here as an altitude below 1000 m) has traversed land northwest of the sampling site during its approach; (ii) *coastal SE* where boundary layer air has traversed land southeast of the sampling site during its approach; (iii) *Pacific Ocean* where boundary layer air has approached directly from the ocean and has not encountered land prior to arrival at the sampling site; and (iv) *free troposphere* where the air mass has spent more than 50 % of the 72 hour back trajectory in the free troposphere. In four sampling periods, back trajectories initiated at different times in the sampling period indicated that the air mass changed during sampling, such as a change in the predominant altitude of the air mass from the free troposphere to the marine boundary layer. In these situations, the air mass category to which the majority of the back trajectories belonged was selected as the air mass category of the sample.

3. Results and discussion

3.1 Back trajectories and the dependence of INP concentrations on air mass classification

Seventy-two hour back trajectories initiated at the midpoint of each INP sampling period are shown in Fig. 2. The back trajectories indicate that 88 % of the air masses sampled spent the majority of their 72 hours prior to reaching the site over the Pacific Ocean within the marine boundary layer (est. < 1000 m). Furthermore, air masses approached the sampling site from an onshore direction with minimal flow over land apart from coastal regions. Average local wind directions of 89° to 297° during INP sampling support this finding. In Fig. S1 of the Supplement, the back trajectories shown in Fig. 2 are color-coded by the classification of the air mass.

Shown in Fig. 3 is the number concentration of INPs as a function of time, color-coded by the classification of the air mass. There is no obvious trend between INP number concentrations and air mass type at temperatures between -15 and -25 °C. At -30 °C, INP number concentrations associated with air masses from the coastal SE (red points) appear to be higher than INP number concentrations associated with other air masses, but the statistics are low for the coastal SE air masses, especially at -30 °C. Figure 4 shows that the mean values for the different air mass types vary by less than a factor of 2.6. We conclude that INP number concentrations did not exhibit a strong dependence on the type of air mass sampled. The correlation analysis presented in Sects. 3.2–3.5 uses the entire dataset (i.e. the data were not differentiated based on air mass type). We further explore the dependence on air mass type in Sect. 3.6.

3.2 Are biological particles a major source of ice nuclei?

To investigate if biological particles are an important source of INPs at the coastal site, we determined correlations between INPs and fluorescent bioparticles. In the following correlation analysis, WIBS-4A data are limited to particle sizes of 10 µm or smaller to better match the size range of the MOUDI-DFT. The correlation coefficients (R) of linear fits to the

data are presented in Table 1 with correlation plots at a freezing temperature of -25 °C shown in Fig. 5 and plots at -15, -20, and -30 °C given in the Supplement. Here we use the scheme of Dancey and Reidy (2011) where correlations with an *R* value of 0.1–0.3, 0.4–0.6, and 0.7–0.9 are classified as weak, moderate, and strong, respectively. In the discussion, correlations with statistical significance (*P* value < 0.05) are emphasized.

With values of *R* between 0.74 and 0.83, INP number concentrations are strongly correlated with the number concentrations of fluorescent bioparticles for INPs active between -15 and -25 °C (Figs. 5a and S3, Table 1). At these temperatures, fluorescent bioparticles have the largest correlation coefficients with INPs compared to all of the other parameters investigated. This suggests that biological particles are an important component of the INP population. Using similar fluorescence techniques, others have also noted strong correlations between INPs and primary biological particles during ambient measurements (Prenni et al., 2009, 2013; Huffman et al., 2013; Tobo et al., 2013).

To further investigate the relationship between biological particles and INPs, we compared the size distributions of INPs with the size distributions of total particles and fluorescent bioparticles, using samples where all three measurements were available. Shown in Fig. 6a–d are the average number concentrations of INPs as a function of particle size for droplet freezing temperatures ranging from -15 to -30 °C. The shapes of all four INP size distributions were nearly identical with a single mode at an aerodynamic diameter of 3.2–5.6 µm.

Also shown in Fig. 6 are the average size distributions of total particles and fluorescent bioparticles as measured with the WIBS-4A over the size range of 0.5–10 µm. As mentioned in Sect. 2.3, due to the decrease in WIBS counting efficiency at particle sizes below approximately 0.7 µm (Healy et al., 2012b), the number concentration of particles sized 0.5–1.0 µm should be

Ryan Mason 10/4/2015 10:47 AM
Deleted: Only correlations with statistical significance (*P* value < 0.05) are discussed.

Ryan Mason 10/4/2015 10:48 AM
Deleted: S1

Ryan Mason 10/4/2015 12:11 PM
Deleted: 6

Ryan Mason 10/4/2015 12:11 PM
Deleted: 7

Ryan Mason 10/4/2015 10:49 AM
Deleted: Due

764 considered a lower limit.

765 The size distribution of total particles (Fig. 6e) was found to be unimodal with the mode
766 at 0.5–1.0 μm. Fluorescent bioparticles were bimodally distributed (Fig. 6f) with one mode at
767 1.8–3.2 μm and another at 0.5–1.0 μm. Figure 6 illustrates that the size distributions of INPs are
768 more closely related to the size distribution of fluorescent bioparticles than total particles,
769 suggesting that biological particles may have had a greater contribution to the INP population
770 than non-biological particles.

771 In addition to the WIBS-4A, the presence of biological material in sampled air was
772 verified by fluorescence microscopy. Images of a sample collected on August 11, 2013 are
773 shown in Fig. 7 as an example. The fraction of particles exhibiting fluorescence on this day
774 based on the WIBS-4A was close to the campaign average value; 7.1 % versus an average of 7.8
775 %. The image here shows a sample containing many biological particles, identified by their blue
776 color which is characteristic of biological fluorophores such as proteins and coenzymes (Pöhlker
777 et al., 2012). Most of these biological particles had a similar morphology with an ellipsoidal
778 shape, approximately 11.9 μm in length × 4.1 μm in width, and multi-nucleation with three
779 septa. Morphologically, many of these appear to be fungal macroconidia, consistent with the
780 physical attributes of ascospores (Carlile et al., 2001; Maheshwari, 2005; Leslie and Summerell,
781 2006; Webster and Weber, 2007). Fungal spores can be ice-active at the temperatures used here
782 (Jayaweera and Flanagan, 1982; Pouleur et al., 1992; Tsumuki et al., 1992; Richard et al., 1996;
783 Iannone et al., 2011; Haga et al., 2013, 2014; Fröhlich-Nowoisky et al., 2015), and the size of the
784 bioparticles observed in Fig. 7 (an estimated aerodynamic diameter of 4.8 μm assuming a prolate
785 spheroid shape and unit density) matches the mode in the INP size distributions of Fig. 6.
786 Predicting the optical diameter that the WIBS-4A would measure for such a particle is difficult,

787 but it is reasonable that they could be detected as slightly larger or smaller depending on the axis
788 upon which the incident light impinges.

789 **3.3 Is black carbon a major source of ice nuclei?**

790 Sources of BC at the sampling site include local marine ship traffic. Atmospheric size
791 distributions obtained at other locations demonstrate that most BC particles are smaller than 1
792 µm (Schwarz et al., 2008, 2013; Schroder et al., 2015). As is shown in Fig. 6, the majority of
793 INPs identified here were larger than 1 µm at all of the temperatures studied. It is therefore likely
794 that BC particles were not the major source of INPs at the sampling site. As correlations between
795 INPs and eBC are moderate at -15 to -25 °C (R = 0.47–0.60, Table 1), we also investigated
796 correlations between INPs and the anthropogenic tracers CO, NO_x, and SO_2. The correlations
797 between INPs and CO, NO_x, and SO_2 are not statistically significant (see Table S2 of the
798 Supplement), further suggesting that BC was not a major INP source.

Ryan Mason 10/4/2015 10:52 AM
Deleted: because their sources, like BC, include fossil fuel combustion and biomass burning (Galanter et al., 2000; Gadi et al., 2003; United States Environmental Protection Agency, 2014)

799 **3.4 Are particles from the ocean a major source of ice nuclei?**

800 Situated in a region of high oceanic primary productivity (Whitney et al., 2005; Ribalet et
801 al., 2010) with onshore winds, particles of marine origin are a potential source of INPs at the
802 sampling site. Therefore, correlations between INP number concentrations and tracers of marine
803 aerosols and marine biological activity were explored. Since primary marine aerosols are ejected
804 from the ocean by the bursting of entrained bubbles (Blanchard and Woodcock, 1957;
805 Blanchard, 1963, 1989; Andreas, 1998), sodium was used as a tracer of primary particles from
806 the ocean. The strength of correlations between INPs and sodium are given in Table 1. Although
807 the correlations range from weakly-to-moderately negative to strongly positive, the large P
808 values (0.20 or greater) indicate that the results are not statistically significant. Due in part to the
809 long sampling times required for the sodium measurements, only three to six data points were

available for the sodium correlation analysis.

MSA is often used as a marker for marine biological productivity (Saltzman et al., 1986; Savoie et al., 1994; Sorooshian et al., 2009; Gaston et al., 2010; Becagli et al., 2013) because it is chemically stable and its precursor, dimethylsulfide, is produced by primary biological activity in the ocean (Andreae et al., 1985; Charlson et al., 1987; Keller, 1989; Bates et al., 1992; Kettle et al., 1999). As INP number concentrations are closely correlated to bioparticles at warmer droplet freezing temperatures, one may expect correlations of a similar magnitude between INPs and MSA if the marine environment was indeed acting as an important source of biological INPs. As is shown in Table 1, no statistically significant correlations are found as *P* values are large (0.15-0.50).

Finally, correlations between wind speed and INP number concentration were investigated using wind speed data from both the site and an offshore buoy. As the dominant source of bubble entrainment in the oceans is breaking waves (O'Dowd and de Leeuw, 2007), the rate of sea-spray production is dependent in part on wind speed. For this correlation, wind speed was first raised to the power of 3.41 using the power law of Monahan and Muircheartaigh (1980) that relates whitecap coverage to wind speed. The correlations found at -30 °C are statistically significant (*P* value < 0.05), but the magnitude of the correlation coefficients is only moderate (*R* = 0.48–0.55; see Table 1). The average wind speed during INP sampling exceeded the onset speed for whitecap formation, approximately 4 m s^{-1} (O'Dowd and de Leeuw, 2007), in only 47 and 56 % of samples when using the lighthouse and buoy data, respectively, and daily observations at the site noted infrequent wave activity. Furthermore, some of the highest INP concentrations were found when the wind speed was less than 4 m s^{-1}. The correlation between local wind direction and INP concentrations was also weak (*R* ranged from -0.19 to -0.32; not

shown).

All correlations between INPs and parameters indicative of marine aerosols and marine biological activity are either moderate at best or not statistically significant. For these reasons, correlations involving sodium, MSA, and wind speed do not provide strong evidence that marine particles were a major contributor to the INP population. Recent measurements have shown the presence of INPs in the sea surface microlayer (Wilson et al., 2015). Our measurements do not contradict these findings since we do not rule out the ocean as a source of INPs. One possibility is that biological INPs released by local vegetation were present in sufficient numbers at this site to overwhelm the presence of any INPs from the ocean.

3.5 What is the major source of ice nuclei active at -30 °C?

At warmer droplet freezing temperatures (-15 to -25 °C), the strongest correlations are observed between number concentrations of fluorescent bioparticles and INPs. In contrast, at -30 °C the strength of correlations between INPs and fluorescent bioparticles and INPs and total particles > 0.5 μm in diameter are equal (R = 0.66; Table 1). It is therefore likely that both biological and non-biological particles were important sources of INPs active at -30 °C. Good correlations between INPs and total particles > 0.5 μm have also been observed in several other field studies (e.g. DeMott et al., 2010; Chou et al., 2011; Field et al., 2012; Prenni et al., 2013; Tobo et al., 2013; Jiang et al., 2015).

Since the INP size distributions of Fig. 6 and the correlations of Table 1 do not provide strong evidence of BC particles or the ocean being a major source of INPs active at -30 °C, it is possible that mineral dust was a major source of INPs as mineral dust particles are known to efficiently nucleate ice at this temperature (e.g. DeMott et al., 2003; Cziczo et al., 2004; Field et al., 2006; Möhler et al., 2006; Marcolli et al., 2007; Zimmermann et al., 2008; Klein et al., 2010;

Niedermeier et al., 2010; Chou et al., 2011; Atkinson et al., 2013; Yakobi-Hancock et al., 2013; Wheeler et al., 2015). The size distribution of INPs did not drastically change between -25 and -30 °C (Fig. 6c and d), and the dominant mode in the surface area distribution of airborne mineral dust (Maring et al., 2003) can occur at approximately the same size range as biological INPs (Després et al., 2012). While in a very different ecosystem and climatic region, Prenni et al. (2009) noted that the relative contribution of mineral dust particles to the total number of INPs in the Amazon region increased as ice nucleation temperature decreased. Only below -27 °C did the amount of mineral dust significantly influence the number of INPs, while above this temperature most INPs were biological (Prenni et al., 2009). Ten-day back trajectories initiated at the midpoint of each INP sampling period are available in Fig. S2 of the Supplement. None of the trajectories pass over major arid regions in Asia or Africa; however, this does not rule out mineral dust or soils as a source of INPs in our measurements.

3.6 Do the potential sources of ice nuclei change with air mass classification?

In the preceding sections we did not differentiate data based on air mass classification. Here we present correlations within each of the four air mass categories introduced in Sect. 2.8 to investigate if the major sources of INPs vary with air mass type. The correlations for each air mass type are given in Table 2. Correlations involving sodium and MSA are not included due to insufficient data, and only statistically significant correlations will be discussed ($P < 0.05$).

The general trends presented in Table 1 for the undifferentiated data are also found in Table 2 for the various air mass categories. In coastal NW, Pacific Ocean, and free tropospheric air masses, INP number concentrations are well correlated to those of fluorescent bioparticles at temperatures between -15 and -25 °C with R values ranging from 0.64 to 0.99 (an average of 0.89), and in free tropospheric air masses a very strong correlation is also found at -30 °C (R =

884 1.00). In most cases, these are the strongest correlations noted at a given temperature. This again
885 suggests that many INPs may have been biological.

886 In coastal NW and free tropospheric air masses, INPs and total particles are also closely
887 correlated. These correlations are strong in the case of coastal NW air masses at ice activation
888 temperatures of -15 to -25 °C (R = 0.70–0.85) and very strong in air masses from the free
889 troposphere between -20 and -30 °C (R = 0.98–0.99). The correlation coefficients are
890 significantly greater than those found in the undifferentiated data of Table 1. With the average
891 fraction of particles that exhibited fluorescence in these air masses being close to the campaign
892 average, the good correlations with total particles suggest that non-biological INPs such as
893 mineral dust may have also contributed to the INP population.

894 Correlations of INPs with eBC are strong (R = 0.71–0.84) at -25 °C and above in coastal
895 NW air masses and very strong (R = 0.99) at -15 °C in air masses from the free troposphere.
896 Correlations of INPs with CO and SO_2 in these air masses are also moderate to very strong in
897 some cases (see Table S3 of the Supplement). However, more than 84 and 100 % of INPs active
898 at these temperatures were larger than 1 μm in size in air masses from the coastal NW and the
899 free troposphere, respectively. Vegetation NW of the sampling site closely follows that of the
900 region, and potential sources of supermicron INPs from the coastal NW include forests of coastal
901 western hemlock. Given the dominance of supermicron INPs in these two air mass types, it is
902 unlikely that BC was an important source of INPs.

903 **3.7 Can existing parameterizations accurately predict measured INP concentrations?**

904 Empirical parameterizations have been developed to predict ice nucleation in atmospheric
905 models. Here we investigate whether or not a number of these parameterizations are consistent
906 with the current measurements. In total we tested six different parameterizations: those of

907 Fletcher (1962), hereafter F62; Cooper (1986), hereafter C86; Meyers et al. (1992), hereafter
908 M92; DeMott et al. (2010), hereafter D10; and two from Tobo et al. (2013), hereafter $T13_{total}$ and
909 $T13_{fluorescent}$. Details on these parameterizations are given in the Supplement.

910 In Fig. 8 we compare measured INP number concentrations with predicted INP number
911 concentrations based on the parameterizations discussed above. The parameterizations of D10,
912 $T13_{total}$ and $T13_{fluorescent}$ require knowledge of either total particle or fluorescent bioparticle
913 number concentrations with sizes > 0.5 µm. Here we use the data from the WIBS-4A over its full
914 size range (0.5–23.7 µm) to better match the sampling conditions used in D10 and T13. Note that
915 the parameterization of $T13_{fluorescent}$ based on fluorescent bioparticle number concentrations was
916 formulated using measurements from an ultraviolet aerodynamic particle sizer (UV-APS),
917 whereas this study uses a WIBS-4A. As noted in Healy et al. (2014), there may be discrepancies
918 between the number concentrations of fluorescent bioparticles detected by the UV-APS and
919 WIBS-4A. With more fluorescent channels and more sensitive electronics, the WIBS-4A may
920 probe different fluorophores than the UV-APS, thus detecting greater concentrations of
921 fluorescent bioparticles and in turn leading to greater predicted INP number concentrations.
922 Also, the INP number concentrations measured by the MOUDI-DFT are for particle sizes of
923 0.18–10 µm, whereas the INP measurements used to formulate the parameterizations of M92,
924 D10, and T13 were for particles ≤ 3, ≤ 1.6, and ≤ 2.4 µm, respectively. As a result, when
925 reporting measured INP number concentrations in Fig. 8 we limit the MOUDI-DFT data to
926 particle sizes that overlap with those used to formulate the parameterizations (see the
927 Supplement for details).

928 It is evident in Fig. 8 that none of the parameterizations are able to consistently predict
929 the measured INP number concentrations within a factor or 5 over the entire temperature range

investigated. The most accurate parameterization is that of C86 (Fig. 8b), predicting 25 % and 57 % of the INP number concentrations within a factor of 2 and 5, respectively, of the solid 1:1 line. While the C86 parameterization works reasonably well at temperatures of -15 to -25 °C, at lower temperatures it becomes increasingly inaccurate, possibly due to it being applied outside the temperature range over which it was developed (-5 to -25 °C).

The parameterizations of D10, $T13_{total}$ and $T13_{fluorescent}$ incorporate measurements of total particles or fluorescent bioparticles, but are found to be poor predictors of the values measured in this study as on average only 41% of INP number concentrations are predicted within a factor of 5 (Fig. 8d–f). A number of datasets from diverse locations were used in the development of the D10 parameterization, but those with a strong marine influence were not included because sea salt is not known to be an efficient ice nucleus under the conditions investigated (immersion freezing at temperatures above -35 °C). Given the proximity of our sampling site to the Pacific Ocean (Fig. 1) and the back trajectories of the sampled air masses (Fig. 2), a marine influence in our samples may contribute to the somewhat poor performance of the D10 parameterization and the over-estimation of INPs shown in Fig. 8d. The $T13_{total}$ and $T13_{fluorescent}$ parameterizations were developed using data from a forested site in Colorado. Differences in the composition, concentration, and ice-nucleating ability of both biological and non-biological particles between the continental forest of T13 and the coastal site of this study may have contributed to the inaccuracy of the $T13_{total}$ and $T13_{fluorescent}$ parameterizations (Fig. 8e–f).

Figure 8 suggests that additional measurements of INPS in other environments, times of year, and altitudes are needed to further test and improve current empirical parameterizations of INPs. The results presented in Fig. 8 also indicate that the application of INP parameterizations

to locations dissimilar to that of the original study used to generate the parameterizations should be done with care.

4. Summary and conclusions

The number concentrations of 0.18–10 μm INPs active in the immersion mode were determined at a coastal site in Western Canada during the summer of 2013 as part of the NETCARE project. We investigated the strength of linear correlations between these INP values and measurements of total particles, fluorescent bioparticles, eBC, sodium, MSA, and wind speed and also compared their size distributions where these measurements were available. We found that (1) biological particles, possibly from local vegetation, were likely the major source of ice nuclei at freezing temperatures between -15 and -25 °C; (2) non-biological particles such as mineral dust may also have had an important contribution to the population of INPs active at -30 °C; (3) the prevalence of supermicron INPs makes BC particles an unlikely source of ice nuclei; and (4) there was no evidence of marine particles being a significant source of ice nuclei, although the ocean as a source of INPs cannot be ruled out. One possibility is that biological INPs released by nearby vegetation were present in sufficient numbers at this site to overwhelm the presence of any INPs from the ocean.

Six empirical parameterizations of ice nucleation for use in atmospheric models were tested to determine the accuracy with which they predict INP number concentrations at this coastal site. Overall, none of the parameterizations were found to be suitable, predicting only 1 to 57 % of INPs within a factor of 5 of the measured value. This highlights the need for the development of INP parameterizations that are appropriate for this complex environment.

In this paper we assumed that particles were externally mixed. In future studies it would be useful to include mixing state measurements together with studies similar to those presented

here to quantify the extent of external versus internal mixing. In addition, studies that identify INPs followed by chemical composition measurements of these particles by electron microscopy (e.g. Knopf et al., 2014) or fluorescence microscopy would be useful to supplement the information gained from correlation analyses of collocated instruments.

Acknowledgements

The authors thank K. Bach, O. Greiner, J. Hansen, A. Klady, K. Love, D. Lovrity, T. Mittertreiner, R. Neagu, P. Padhiar for designing and constructing the NETCARE mobile laboratory used in this study, A. Chivulescu for assistance with ion chromatography measurements, D. O'Connor for assistance analyzing and interpreting WIBS-4A measurements, and L. A. Miller for helpful discussions. The sampling site at Amphitrite Point is located at a Coast Guard station and we would like to thank the Department of Fisheries and Oceans and all the staff at the site for their help. The site is jointly supported and maintained by Environment Canada, the British Columbia Ministry of Environment, and Metro Vancouver. The Natural Sciences and Engineering Research Council of Canada supported this research through its Climate Change and Atmospheric Research program. The authors gratefully acknowledge the NOAA Air Resources Laboratory (ARL) for the provision of the HYSPLIT transport and dispersion model and READY website (http://www.ready.noaa.gov) used in this publication. J. A. Huffman and J. Li acknowledge internal faculty support from the Division of Natural Sciences and Math and PROF grant support from the Office of Research and Sponsored Programs at the University of Denver.

997 **References**

998 Alpert, P. A., Aller, J. Y. and Knopf, D. A.: Ice nucleation from aqueous NaCl droplets with and
999 without marine diatoms, Atmos. Chem. Phys., 11, 5539–5555, doi:10.5194/acp-11-5539-2011,
1000 2011.

1001 Andreae, M. O., Ferek, R. J., Bermond, F., Byrd, K. P., Engstrom, R. T., Hardin, S., Houmere, P.
1002 D., LeMarrec, F., Raemdonck, H. and Chatfield, R. B.: Dimethyl sulfide in the marine
1003 atmosphere, J. Geophys. Res., 90, 12891–12900, doi:10.1029/JD090iD07p12891, 1985.

1004 Andreas, E. L.: A New Sea Spray Generation Function for Wind Speeds up to 32 m s^{-1}, J. Phys.
1005 Oceanogr., 28, 2175–2184, 1998.

1006 Atkinson, J. D., Murray, B. J., Woodhouse, M. T., Whale, T. F., Baustian, K. J., Carslaw, K. S.,
1007 Dobbie, S., O'Sullivan, D. and Malkin, T. L.: The importance of feldspar for ice nucleation by
1008 mineral dust in mixed-phase clouds, Nature, 498, 355–358, doi:10.1038/nature12278, 2013.

1009 Augustin, S., Wex, H., Niedermeier, D., Pummer, B., Grothe, H., Hartmann, S., Tomsche, L.,
1010 Clauss, T., Voigtländer, J., Ignatius, K. and Stratmann, F.: Immersion freezing of birch pollen
1011 washing water, Atmos. Chem. Phys., 13, 10989–11003, doi:10.5194/acp-13-10989-2013, 2013.

1012 Austin, M. A., Buffet, D. A., Nicholson, D. J. and Scudder, G. G. E.: Taking Natures Pulse: The
1013 Status of Biodiversity in British Columbia, Biodiversity BC, Victoria, available at:
1014 http://www.biodiversitybc.org (last access: 10 October 2014), 2008.

1015 Baker, M. B.: Cloud Microphysics and Climate, Science, 276, 1072–1078,
1016 doi:10.1126/science.276.5315.1072, 1997.

1017 Bates, T. S., Calhoun, J. A. and Quinn, P. K.: Variations in the methanesulfonate to sulfate molar
1018 ratio in submicrometer marine aerosol particles over the South Pacific Ocean, J. Geophys. Res.
1019 Ocean., 97, 9859–9865, doi:10.1029/92JD00411, 1992.

1020 Becagli, S., Lazzara, L., Fani, F., Marchese, C., Traversi, R., Severi, M., di Sarra, A., Sferlazzo,
1021 D., Piacentino, S., Bommarito, C., Dayan, U. and Udisti, R.: Relationship between
1022 methanesulfonate (MS^-) in atmospheric particulate and remotely sensed phytoplankton activity in
1023 oligo-mesotrophic central Mediterranean Sea, Atmos. Environ., 79, 681–688,
1024 doi:10.1016/j.atmosenv.2013.07.032, 2013.

1025 Blanchard, D. C.: The electrification of the atmosphere by particles from bubbles in the sea,
1026 Prog. Oceanogr., 1, 73–202, doi:10.1016/0079-6611(63)90004-1, 1963.

1027 Blanchard, D. C.: The ejection of drops from the sea and their enrichment with bacteria and other
1028 materials: A review, Estuaries, 12, 127–137, doi:10.2307/1351816, 1989.

1029 Blanchard, D. C. and Woodcock, A. H.: Bubble formation and modification in the sea and its
1030 meteorological significance, Tellus, 9, 145–158, doi:10.1111/j.2153-3490.1957.tb01867.x, 1957.

1031 Bones, D. L., Henricksen, D. K., Mang, S. A., Gonsior, M., Bateman, A. P., Nguyen, T. B.,
1032 Cooper, W. J. and Nizkorodov, S. A.: Appearance of strong absorbers and fluorophores in
1033 limonene-O_3 secondary organic aerosol due to NH_4^+-mediated chemical aging over long time
1034 scales, J. Geophys. Res., 115, D05203, doi:10.1029/2009JD012864, 2010.

1035 Boucher, O., Randall, D., Artaxo, P., Bretherton, C., Feingold, G., Foster, P., Kerminen, V.-M.,
1036 Kondo, Y., Liao, H., Lohmann, U., Rasch, P., Satheesh, S. K., Sherwood, S., Stevens, B. and
1037 Zhang, X. Y.: Clouds and Aerosols, in Climate Change 2013: The Physical Science Basis.
1038 Contribution of Working Group I to the Fifth Assessment Report of the Intergovernmental Panel
1039 on Climate Change, edited by T. F. Stocker, D. Qin, G.-K. Plattner, M. Tignor, S. K. Allen, J.
1040 Boschung, A. Nauels, Y. Xia, V. Bex, and P. M. Midgley, Cambridge University Press,
1041 Cambridge, United Kingdom and New York, NY, USA, 2013.

1042 Broadley, S. L., Murray, B. J., Herbert, R. J., Atkinson, J. D., Dobbie, S., Malkin, T. L.,
1043 Condliffe, E. and Neve, L.: Immersion mode heterogeneous ice nucleation by an illite rich
1044 powder representative of atmospheric mineral dust, Atmos. Chem. Phys., 12, 287–307,
1045 doi:10.5194/acp-12-287-2012, 2012.

1046 Brooks, S. D., Suter, K. and Olivarez, L.: Effects of Chemical Aging on the Ice Nucleation
1047 Activity of Soot and Polycyclic Aromatic Hydrocarbon Aerosols, J. Phys. Chem. A, 118, 10036–
1048 10047, doi:10.1021/jp508809y, 2014.

1049 Burrows, S. M., Hoose, C., Pöschl, U. and Lawrence, M. G.: Ice nuclei in marine air: biogenic
1050 particles or dust?, Atmos. Chem. Phys., 13, 245–267, doi:10.5194/acp-13-245-2013, 2013.

1051 Carlile, M. J., Watkinson, S. C. and Gooday, G. W.: The Fungi, Second Edi., Academic Press,
1052 London, United Kingdom and San Diego, CA, USA, 2001.

1053 Charlson, R. J., Lovelock, J. E., Andreae, M. O. and Warren, S. G.: Oceanic phytoplankton,
1054 atmospheric sulphur, cloud albedo and climate, Nature, 326, 655–661, doi:10.1038/326655a0,
1055 1987.

1056 Chou, C., Stetzer, O., Weingartner, E., Jurányi, Z., Kanji, Z. A. and Lohmann, U.: Ice nuclei
1057 properties within a Saharan dust event at the Jungfraujoch in the Swiss Alps, Atmos. Chem.
1058 Phys., 11, 4725–4738, doi:10.5194/acp-11-4725-2011, 2011.

1059 Christner, B. C., Morris, C. E., Foreman, C. M., Cai, R. and Sands, D. C.: Ubiquity of Biological
1060 Ice Nucleators in Snowfall, Science, 319, 1214, doi:10.1126/science.1149757, 2008.

1061 Conen, F., Morris, C. E., Leifeld, J., Yakutin, M. V and Alewell, C.: Biological residues define
1062 the ice nucleation properties of soil dust, Atmos. Chem. Phys., 11, 9643–9648, doi:10.5194/acp-
1063 11-9643-2011, 2011.

1064 Cooper, W. A.: Ice initiation in natural clouds, Meteor. Mon., 21, 29–32, doi:10.1175/0065-
1065 9401-21.43.29, 1986.

1066 Corbin, J. C., Rehbein, P. J. G., Evans, G. J. and Abbatt, J. P. D.: Combustion particles as ice
1067 nuclei in an urban environment: Evidence from single-particle mass spectrometry, Atmos.
1068 Environ., 51, 286–292, doi:10.1016/j.atmosenv.2012.01.007, 2012.

1069 Costa, T. S., Gonçalves, F. L. T., Yamasoe, M. A., Martins, J. A. and Morris, C. E.: Bacterial ice
1070 nuclei impact cloud lifetime and radiative properties and reduce atmospheric heat loss in the
1071 BRAMS simulation model, Environ. Res. Lett., 9, 084020, doi:10.1088/1748-9326/9/8/084020,
1072 2014.

1073 Cozic, J., Mertes, S., Verheggen, B., Cziczo, D. J., Gallavardin, S. J., Walter, S., Baltensperger,
1074 U. and Weingartner, E.: Black carbon enrichment in atmospheric ice particle residuals observed

1075 in lower tropospheric mixed phase clouds, J. Geophys. Res., 113, D15209,
1076 doi:10.1029/2007JD009266, 2008.

1077 Creamean, J. M., Suski, K. J., Rosenfeld, D., Cazorla, A., DeMott, P. J., Sullivan, R. C., White,
1078 A. B., Ralph, F. M., Minnis, P., Comstock, J. M., Tomlinson, J. M. and Prather, K. A.: Dust and
1079 Biological Aerosols from the Sahara and Asia Influence Precipitation in the Western U.S.,
1080 Science, 339, 1572–1578, doi:10.1126/science.1227279, 2013.

1081 Cziczo, D. J., Froyd, K. D., Hoose, C., Jensen, E. J., Diao, M., Zondlo, M. A., Smith, J. B.,
1082 Twohy, C. H. and Murphy, D. M.: Clarifying the Dominant Sources and Mechanisms of Cirrus
1083 Cloud Formation, Science, 340, 1320–1324, doi:10.1126/science.1234145, 2013.

1084 Cziczo, D. J., Murphy, D. M., Hudson, P. K. and Thomson, D. S.: Single particle measurements
1085 of the chemical composition of cirrus ice residue during CRYSTAL-FACE, J. Geophys. Res.,
1086 109, D04201, doi:10.1029/2003JD004032, 2004.

1087 Dancey, C. P. and Reidy, J.: Statistics Without Maths for Psychology, Pearson Education
1088 Limited, Essex, England, 2011.

1089 DeMott, P. J., Hill, T. C. J., McCluskey, C. S., Prather, K. A., Collins, D. B., Sullivan, R. C.,
1090 Ruppel, M. J., Mason, R. H., Irish, V. E., Lee, T., Hwang, C. Y., Rhee, T. S., Snider, J. R.,
1091 McMeeking, G. R., Dhaniyala, S., Lewis, E. R., Wentzell, J., Abbatt, J. P. D., Lee, C., Sultana,
1092 C. M., Ault, A. P., Axson, J. I., Martinez, M. D., Venero, I., Figueroa, G. S., Stokes, M. D.,
1093 Deane, G. B., Mayol-Bracero, O. L., Grassian, V. H., Bertram, T. H., Bertram, A. K., Moffett, B.
1094 F. and Franc, G. D.: Sea spray aerosol as a unique source of ice nucleating particles, submitted,
1095 2015.

1096 DeMott, P. J., Petters, M. D., Prenni, A. J., Carrico, C. M., Kreidenweis, S. M., Collett Jr., J. L.
1097 and Moosmüller, H.: Ice nucleation behavior of biomass combustion particles at cirrus
1098 temperatures, J. Geophys. Res., 114, D16205, doi:10.1029/2009JD012036, 2009.

1099 DeMott, P. J., Prenni, A. J., Liu, X., Kreidenweis, S. M., Petters, M. D., Twohy, C. H.,
1100 Richardson, M. S., Eidhammer, T. and Rogers, D. C.: Predicting global atmospheric ice nuclei
1101 distributions and their impacts on climate, P. Natl. Acad. Sci. USA, 107, 11217–11222,
1102 doi:10.1073/pnas.0910818107, 2010.

1103 DeMott, P. J., Sassen, K., Poellot, M. R., Baumgardner, D., Rogers, D. C., Brooks, S. D., Prenni,
1104 A. J. and Kreidenweis, S. M.: African dust aerosols as atmospheric ice nuclei, Geophys. Res.
1105 Lett., 30, 1732, doi:10.1029/2003GL017410, 2003.

1106 Després, V. R., Huffman, J. A., Burrows, S. M., Hoose, C., Safatov, A. S., Buryak, G., Fröhlich-
1107 Nowoisky, J., Elbert, W., Andreae, M. O., Pöschl, U. and Jaenicke, R.: Primary biological
1108 aerosol particles in the atmosphere: a review, Tellus B, 64, 15598,
1109 doi:10.3402/tellusb.v64i0.15598, 2012.

1110 Diehl, K., Matthias-Maser, S., Jaenicke, R. and Mitra, S. K.: The ice nucleating ability of pollen:
1111 Part II. Laboratory studies in immersion and contact freezing modes, Atmos. Res., 61, 125–133,
1112 doi:10.1016/S0169-8095(01)00132-6, 2002.

1113 Diehl, K., Quick, C., Matthias-Maser, S., Mitra, S. K. and Jaenicke, R.: The ice nucleating ability
1114 of pollen: Part I. Laboratory studies in deposition and condensation freezing modes, Atmos. Res.,
1115 58, 75–87, doi:10.1016/S0169-8095(01)00091-6, 2001.

1116 Draxler, R. R. and Rolph, G. D.: HYSPLIT (HYbrid Single-Particle Lagrangian Integrated
1117 Trajectory) Model access via NOAA ARL READY Website, available at:
1118 http://ready.arl.noaa.gov/HYSPLIT.php (last access: 27 May 2014), NOAA Air Resources
1119 Laboratory, Silver Spring, MD, 2014.

1120 Dymarska, M., Murray, B. J., Sun, L., Eastwood, M. L., Knopf, D. A. and Bertram, A. K.:
1121 Deposition ice nucleation on soot at temperatures relevant for the lower troposphere, J. Geophys.
1122 Res., 111, D04204, doi:10.1029/2005JD006627, 2006.

1123 Ebert, M., Worringen, A., Benker, N., Mertes, S., Weingartner, E. and Weinbruch, S.: Chemical
1124 composition and mixing-state of ice residuals sampled within mixed phase clouds, Atmos.
1125 Chem. Phys., 11, 2805–2816, doi: 10.5194/acp-11-2805-2011, 2011.

1126 Field, P. R., Heymsfield, A. J., Shipway, B. J., DeMott, P. J., Pratt, K. A., Rogers, D. C., Stith, J.
1127 and Prather, K. A.: Ice in Clouds Experiment-Layer Clouds. Part II: Testing Characteristics of
1128 Heterogeneous Ice Formation in Lee Wave Clouds, J. Atmos. Sci., 69, 1066–1079,
1129 doi:10.1175/JAS-D-11-026.1, 2012.

1130 Field, P. R., Möhler, O., Connolly, P., Krämer, M., Cotton, R., Heymsfield, A. J., Saathoff, H.
1131 and Schnaiter, M.: Some ice nucleation characteristics of Asian and Saharan desert dust, Atmos.
1132 Chem. Phys., 6, 2991–3006, doi:10.5194/acp-6-2991-2006, 2006.

1133 Fletcher, N. H.: The Physics of Rainclouds, Cambridge University Press, Cambridge, United
1134 Kingdom, 1962.

1135 Friedman, B., Kulkarni, G., Beránek, J., Zelenyuk, A., Thornton, J. A. and Cziczo, D. J.: Ice
1136 nucleation and droplet formation by bare and coated soot particles, J. Geophys. Res., 116,
1137 D17203, doi:10.1029/2011JD015999, 2011.

1138 Fröhlich-Nowoisky, J., Hill, T. C. J., Pummer, B. G., Yordanova, P., Franc, G. D. and Pöschl,
1139 U.: Ice nucleation activity in the widespread soil fungus *Mortierella alpina*, Biogeosciences, 12,
1140 1057–1071, doi:10.5194/bg-12-1057-2015, 2015.

1141 Gabey, A. M., Gallagher, M. W., Whitehead, J., Dorsey, J. R., Kaye, P. H. and Stanley, W. R.:
1142 Measurements and comparison of primary biological aerosol above and below a tropical forest
1143 canopy using a dual channel fluorescence spectrometer, Atmos. Chem. Phys., 10, 4453–4466,
1144 doi:10.5194/acp-10-4453-2010, 2010.

1145 Gabey, A. M., Stanley, W. R., Gallagher, M. W. and Kaye, P. H.: The fluorescence properties of
1146 aerosol larger than 0.8 μm in urban and tropical rainforest locations, Atmos. Chem. Phys., 11,
1147 5491–5504, doi:10.5194/acp-11-5491-2011, 2011.

1148 Gadi, R., Kulshrestha, U. C., Sarkar, A. K., Garg, S. C. and Parashar, D. C.: Emissions of SO_2
1149 and NO_x from biofuels in India, Tellus B, 55, 787–795, doi:10.1034/j.1600-0889.2003.00065.x,
1150 2003.

1151 Galanter, M., Levy II, H. and Carmichael, G. R.: Impacts of biomass burning on tropospheric
1152 CO, NO_x, and O_3, J. Geophys. Res., 105, 6633–6653, doi:10.1029/1999JD901113, 2000.

1153 Garcia, E., Hill, T. C. J., Prenni, A. J., DeMott, P. J., Franc, G. D. and Kreidenweis, S. M.:
1154 Biogenic ice nuclei in boundary layer air over two U.S. High Plains agricultural regions, J.
1155 Geophys. Res., 117, D18209, doi:10.1029/2012JD018343, 2012.

Gaston, C. J., Pratt, K. A., Qin, X. and Prather, K. A.: Real-Time Detection and Mixing State of Methanesulfonate in Single Particles at an Inland Urban Location during a Phytoplankton Bloom, Environ. Sci. Technol., 44, 1566–1572, doi:10.1021/es902069d, 2010.

Gorbunov, B., Baklanov, A., Kakutkina, N., Windsor, H. L. and Toumi, R.: Ice nucleation on soot particles, J. Aerosol Sci., 32, 199–215, doi:10.1016/s0021-8502(00)00077-x, 2001.

Hader, J. D., Wright, T. P. and Petters, M. D.: Contribution of pollen to atmospheric ice nuclei concentrations, Atmos. Chem. Phys., 14, 5433–5449, doi:10.5194/acp-14-5433-2014, 2014.

Haga, D. I., Burrows, S. M., Iannone, R., Wheeler, M. J., Mason, R. H., Chen, J., Polishchuk, E. A., Pöschl, U. and Bertram, A. K.: Ice nucleation by fungal spores from the classes *Agaricomycetes*, *Ustilaginomycetes*, and *Eurotiomycetes*, and the effect on the atmospheric transport of these spores, Atmos. Chem. Phys., 14, 8611–8630, doi:10.5194/acp-14-8611-2014, 2014.

Haga, D. I., Iannone, R., Wheeler, M. J., Mason, R., Polishchuk, E. A., Fetch Jr., T., van der Kamp, B. J., McKendry, I. G. and Bertram, A. K.: Ice nucleation properties of rust and bunt fungal spores and their transport to high altitudes, where they can cause heterogeneous freezing, J. Geophys. Res.-Atmos., 118, 7260–7272, doi:10.1002/jgrd.50556, 2013.

Healy, D. A., Huffman, J. A., O'Connor, D. J., Pöhlker, C., Pöschl, U. and Sodeau, J. R.: Ambient measurements of biological aerosol particles near Killarney, Ireland: a comparison between real-time fluorescence and microscopy techniques, Atmos. Chem. Phys., 14, 8055–8069, doi:10.5194/acp-14-8055-2014, 2014.

Healy, D. A., O'Connor, D. J., Burke, A. M. and Sodeau, J. R.: A laboratory assessment of the Waveband Integrated Bioaerosol Sensor (WIBS-4) using individual samples of pollen and fungal spore material, Atmos. Environ., 60, 534–543, doi:10.1016/j.atmosenv.2012.06.052, 2012a.

Healy, D. A., O'Connor, D. J. and Sodeau, J. R.: Measurement of the particle counting efficiency of the "Waveband Integrated Bioaerosol Sensor" model number 4 (WIBS-4), J. Aerosol Sci., 47, 94–99, doi:10.1016/j.jaerosci.2012.01.003, 2012b.

Hill, T. C. J., Moffett, B. F., DeMott, P. J., Georgakopoulos, D. G., Stump, W. L. and Franc, G. D.: Measurement of Ice Nucleation-Active Bacteria on Plants and in Precipitation by Quantitative PCR, Appl. Environ. Microbiol., 80, 1256–1267, doi: 10.1128/AEM.02967-13, 2014.

Hiranuma, N., Möhler, O., Yamashita, K., Tajiri, T., Saito, A., Kiselev, A., Hoffmann, N., Hoose, C., Jantsch, E., Koop, T. and Murakami, M.: Ice nucleation by cellulose and its potential contribution to ice formation in clouds, Nat. Geosci., 8, 273–277, doi:10.1038/ngeo2374, 2015.

Hoose, C., Kristjánsson, J. E. and Burrows, S. M.: How important is biological ice nucleation in clouds on a global scale?, Environ. Res. Lett., 5, 024009, doi:10.1088/1748-9326/5/2/024009, 2010a.

Hoose, C., Kristjánsson, J. E., Chen, J.-P. and Hazra, A.: A Classical-Theory-Based Parameterization of Heterogeneous Ice Nucleation by Mineral Dust, Soot, and Biological Particles in a Global Climate Model, J. Atmos. Sci., 67, 2483–2503, doi:10.1175/2010JAS3425.1, 2010b.

1196 Hoose, C. and Möhler, O.: Heterogeneous ice nucleation on atmospheric aerosols: a review of
1197 results from laboratory experiments, Atmos. Chem. Phys., 12, 9817–9854, doi:10.5194/acp-12-
1198 9817-2012, 2012.

1199 Huffman, J. A., Prenni, A. J., DeMott, P. J., Pöhlker, C., Mason, R. H., Robinson, N. H.,
1200 Fröhlich-Nowoisky, J., Tobo, Y., Després, V. R., Garcia, E., Gochis, D. J., Harris, E., Müller-
1201 Germann, I., Ruzene, C., Schmer, B., Sinha, B., Day, D. A., Andreae, M. O., Jimenez, J. L.,
1202 Gallagher, M., Kreidenweis, S. M., Bertram, A. K. and Pöschl, U.: High concentrations of
1203 biological aerosol particles and ice nuclei during and after rain, Atmos. Chem. Phys., 13, 6151–
1204 6164, doi:10.5194/acp-13-6151-2013, 2013.

1205 Huffman, J. A., Sinha, B., Garland, R. M., Snee-Pollmann, A., Gunthe, S. S., Artaxo, P., Martin,
1206 S. T., Andreae, M. O. and Pöschl, U.: Size distributions and temporal variations of biological
1207 aerosol particles in the Amazon rainforest characterized by microscopy and real-time UV-APS
1208 fluorescence techniques during AMAZE-08, Atmos. Chem. Phys., 12, 11997–12019,
1209 doi:10.5194/acp-12-11997-2012, 2012.

1210 Huffman, J. A., Treutlein, B. and Pöschl, U.: Fluorescent biological aerosol particle
1211 concentrations and size distributions measured with an Ultraviolet Aerodynamic Particle Sizer
1212 (UV-APS) in Central Europe, Atmos. Chem. Phys., 10, 3215–3233, doi:10.5194/acp-10-3215-
1213 2010, 2010.

1214 Iannone, R., Chernoff, D. I., Pringle, A., Martin, S. T. and Bertram, A. K.: The ice nucleation
1215 ability of one of the most abundant types of fungal spores found in the atmosphere, Atmos.
1216 Chem. Phys., 11, 1191–1201, doi:10.5194/acp-11-1191-2011, 2011.

1217 Jayaweera, K. and Flanagan, P.: Investigations on biogenic ice nuclei in the Arctic atmosphere,
1218 Geophys. Res. Lett., 9, 94–97, doi:10.1029/GL009i001p00094, 1982.

1219 Jiang, H., Yin, Y., Su, H., Shan, Y. and Gao, R.: The characteristics of atmospheric ice nuclei
1220 measured at the top of Huangshan (the Yellow Mountains) in Southeast China using a newly
1221 built static vacuum water vapor diffusion chamber, Atmos. Res., 153, 200–208,
1222 doi:10.1016/j.atmosres.2014.08.015, 2015.

1223 Joly, M., Amato, P., Deguillaume, L., Monier, M., Hoose, C. and Delort, A.-M.: Quantification
1224 of ice nuclei active at near 0 °C temperatures in low-altitude clouds at the Puy de Dôme
1225 atmospheric station, Atmos. Chem. Phys., 14, 8185–8195, doi:10.5194/acp-14-8185-2014, 2014.

1226 Kamphus, M., Ettner-Mahl, M., Klimach, T., Drewnick, F., Keller, L., Cziczo, D. J., Mertes, S.,
1227 Borrmann, S. and Curtius, J.: Chemical composition of ambient aerosol, ice residues and cloud
1228 droplet residues in mixed-phase clouds: single particle analysis during the Cloud and Aerosol
1229 Characterization Experiment (CLACE 6), Atmos. Chem. Phys., 10, 8077–8095,
1230 doi:10.5194/acp-10-8077-2010, 2010.

1231 Kanji, Z. A. and Abbatt, J. P. D.: Ice Nucleation onto Arizona Test Dust at Cirrus Temperatures:
1232 Effect of Temperature and Aerosol Size on Onset Relative Humidity, J. Phys. Chem. A, 114,
1233 935–941, doi:10.1021/jp908661m, 2010.

1234 Kärcher, B., Möhler, O., DeMott, P. J., Pechtl, S. and Yu, F.: Insights into the role of soot
1235 aerosols in cirrus cloud formation, Atmos. Chem. Phys., 7, 4203–4227, doi:10.5194/acp-7-4203-
1236 2007, 2007.

1237 Kaye, P., Stanley, W. R., Hirst, E., Foot, E. V, Baxter, K. L. and Barrington, S. J.: Single particle
1238 multichannel bio-aerosol fluorescence sensor, Opt. Express, 13, 3583–3593,
1239 doi:10.1364/OPEX.13.003583, 2005.

1240 Keller, M. D.: Dimethyl Sulfide Production and Marine Phytoplankton: The Importance of
1241 Species Composition and Cell Size, Biol. Oceanogr., 6, 375–382,
1242 doi:10.1080/01965581.1988.10749540, 1989.

1243 Kettle, A. J., Andreae, M. O., Amouroux, D., Andreae, T. W., Bates, T. S., Berresheim, H.,
1244 Bingemer, H., Boniforti, R., Curran, M., DiTullio, G. R., Helas, G., Jones, G. B., Keller, M. D.,
1245 Kiene, R. P., Leck, C., Levasseur, M., Malin, G., Maspero, M., Matrai, P., McTaggart, A. R.,
1246 Mihalopoulos, N., Nguyen, B. C., Novo, A., Putaud, J. P., Rapsomanikis, S., Roberts, G.,
1247 Schebeske, G., Sharma, S., Simó, R., Staubes, R., Turner, S. and Uher, G.: A global database of
1248 sea surface dimethylsulfide (DMS) measurements and a procedure to predict sea surface DMS as
1249 a function of latitude, longitude, and month, Glob. Biogeochem. Cy., 13, 399–444,
1250 doi:10.1029/1999GB900004, 1999.

1251 Klein, H., Nickovic, S., Haunold, W., Bundke, U., Nillius, B., Ebert, M., Weinbruch, S., Schuetz,
1252 L., Levin, Z., Barrie, L. A. and Bingemer, H.: Saharan dust and ice nuclei over Central Europe,
1253 Atmos. Chem. Phys., 10, 10211–10221, doi:10.5194/acp-10-10211-2010, 2010.

1254 Knopf, D. A., Alpert, P. A., Wang, B. and Aller, J. Y.: Stimulation of ice nucleation by marine
1255 diatoms, Nat. Geosci., 4, 88–90, doi:10.1038/ngeo1037, 2011.

1256 Knopf, D. A., Alpert, P. A., Wang, B., O'Brien, R. E., Kelly, S. T., Laskin, A., Gilles, M. K. and
1257 Moffet, R. C.: Microspectroscopic imaging and characterization of individually identified ice
1258 nucleating particles from a case field study, J. Geophys. Res.-Atmos., 119, 10365–10381,
1259 doi:10.1002/2014JD021866, 2014.

1260 Knopf, D. A. and Koop, T.: Heterogeneous nucleation of ice on surrogates of mineral dust, J.
1261 Geophys. Res., 111, D12201, doi:10.1029/2005JD006894, 2006.

1262 Koop, T., Kapilashrami, A., Molina, L. T. and Molina, M. J.: Phase transitions of sea-salt/water
1263 mixtures at low temperatures: Implications for ozone chemistry in the polar marine boundary
1264 layer, J. Geophys. Res., 105, 26393–26402, doi:10.1029/2000JD900413, 2000.

1265 Koop, T., Luo, B., Biermann, U. M., Crutzen, P. J. and Peter, T.: Freezing of $HNO_3/H_2SO_4/H_2O$
1266 solutions at stratospheric temperatures: Nucleation statistics and experiments, J. Phys. Chem. A,
1267 101, 1117–1133, doi:10.1021/jp9626531, 1997.

1268 Kottek, M., Grieser, J., Beck, C., Rudolf, B. and Rubel, F.: World Map of the Köppen-Geiger
1269 climate classification updated, Meteorol. Z., 15, 259–263, doi:10.1127/0941-2948/2006/0130,
1270 2006.

1271 Kozloff, L. M., Schofield, M. A. and Lute, M.: Ice nucleating activity of Pseudomonas syringae
1272 and Erwinia herbicola, J. Bacteriol., 153, 222–231, 1983.

1273 Kulkarni, G. and Dobbie, S.: Ice nucleation properties of mineral dust particles: determination of
1274 onset RH_i, IN active fraction, nucleation time-lag, and the effect of active sites on contact angles,
1275 Atmos. Chem. Phys., 10, 95–105, doi:10.5194/acp-10-95-2010, 2010.

Lee, H. J., Laskin, A., Laskin, J. and Nizkorodov, S. A.: Excitation-Emission Spectra and Fluorescence Quantum Yields for Fresh and Aged Biogenic Secondary Organic Aerosols, Environ. Sci. Technol., 47, 5763–5770, doi:10.1021/es400644c, 2013.

Leslie, J. F. and Summerell, B. A.: The *Fusarium* Laboratory Manual, Blackwell Publishing, Ames, Iowa, USA, 2006.

Lin, J. C., Matsui, T., Pielke Sr., R. A. and Kummerow, C.: Effects of biomass-burning-derived aerosols on precipitation and clouds in the Amazon Basin: a satellite-based empirical study, J. Geophys. Res., 111, D19204, doi:10.1029/2005JD006884, 2006.

Lindow, S. E., Arny, D. C. and Upper, C. D.: Erwinia herbicola: A Bacterial Ice Nucleus Active in Increasing Frost Injury to Corn, Phytopathology, 68, 523–527, 1978.

Liu, X., Penner, J. E. and Wang, M.: Influence of anthropogenic sulfate and black carbon on upper tropospheric clouds in the NCAR CAM3 model coupled to the IMPACT global aerosol model, J. Geophys. Res., 114, D03204, doi:10.1029/2008JD010492, 2009.

Lohmann, U.: A glaciation indirect aerosol effect caused by soot aerosols, Geophys. Res. Lett., 29, 1052, doi:10.1029/2001GL014357, 2002.

Lüönd, F., Stetzer, O., Welti, A. and Lohmann, U.: Experimental study on the ice nucleation ability of size-selected kaolinite particles in the immersion mode, J. Geophys. Res., 115, D14201, doi:10.1029/2009JD012959, 2010.

Maheshwari, R.: Fungi: Experimental Methods in Biology, CRC Press, Taylor & Francis Group, Boca Raton, Florida, USA, 2005.

Maki, L. R., Galyan, E. L., Chang-Chien, M.-M. and Caldwell, D. R.: Ice nucleation induced by pseudomonas syringae, Appl. Microbiol., 28, 456–459, 1974.

Maki, L. R. and Willoughby, K. J.: Bacteria as Biogenic Sources of Freezing Nuclei, J. Appl. Meteorol., 17, 1049–1053, 1978.

Marcolli, C., Gedamke, S., Peter, T. and Zobrist, B.: Efficiency of immersion mode ice nucleation on surrogates of mineral dust, Atmos. Chem. Phys., 7, 5081–5091, doi:10.5194/acp-7-5081-2007, 2007.

Maring, H., Savoie, D. L., Izaguirre, M. A., Custals, M. and Reid, J. S.: Mineral dust aerosol size distribution change during atmospheric transport, J. Geophys. Res., 108, 8592, doi:10.1029/2002JD002536, 2003.

Marple, V. A., Rubow, K. L. and Behm, S. M.: A Microorifice Uniform Deposit Impactor (MOUDI): Description, Calibration, and Use, Aerosol Sci. Technol., 14, 434–446, doi:10.1080/02786829108959504, 1991.

Mason, B. J. and Maybank, J.: Ice-nucleating properties of some natural mineral dusts, Q. J. R. Meteorol. Soc., 84, 235–241, doi:10.1002/qj.49708436104, 1958.

Mason, R. H., Chou, C., McCluskey, C. S., Levin, E. J. T., Schiller, C. L., Hill, T. C. J., Huffman, J. A., DeMott, P. J. and Bertram, A. K.: The micro-orifice uniform deposit impactor-droplet freezing technique (MOUDI-DFT) for measuring concentrations of ice nucleating particles as a function of size: improvements and initial validation, Atmos. Meas. Tech., 8, 2449–2462, doi:10.5194/amt-8-2449-2015, 2015.

McCluskey, C. S., DeMott, P. J., Prenni, A. J., Levin, E. J. T., McMeeking, G. R., Sullivan, A. P., Hill, T. C. J., Nakao, S., Carrico, C. M. and Kreidenweis, S. M.: Characteristics of atmospheric ice nucleating particles associated with biomass burning in the US: Prescribed burns and wildfires, J. Geophys. Res.-Atmos., 119, 10458–10470, doi:10.1002/2014JD021980, 2014.

McKendry, I. G., Christensen, E., Schiller, C. L., Vingarzan, R., Macdonald, A. M. and Li, Y.: Low Ozone Episodes at Amphitrite Point Marine Boundary Layer Observatory, British Columbia, Canada, Atmosphere-Ocean, 52, 271–280, doi:10.1080/07055900.2014.910164, 2014.

Meyers, M. P., DeMott, P. J. and Cotton, W. R.: New primary ice-nucleation parameterizations in an explicit cloud model, J. Appl. Meteorol., 31, 708–721, 1992.

Möhler, O., Büttner, S., Linke, C., Schnaiter, M., Saathoff, H., Stetzer, O., Wagner, R., Krämer, M., Mangold, A., Ebert, V. and Schurath, U.: Effect of sulfuric acid coating on heterogeneous ice nucleation by soot aerosol particles, J. Geophys. Res., 110, D11210, doi:10.1029/2004JD005169, 2005.

Möhler, O., DeMott, P. J., Vali, G. and Levin, Z.: Microbiology and atmospheric processes: the role of biological particles in cloud physics, Biogeosciences, 4, 1059–1071, doi:10.5194/bg-4-1059-2007, 2007.

Möhler, O., Field, P. R., Connolly, P., Benz, S., Saathoff, H., Schnaiter, M., Wagner, R., Cotton, R., Krämer, M., Mangold, A. and Heymsfield, A. J.: Efficiency of the deposition mode ice nucleation on mineral dust particles, Atmos. Chem. Phys., 6, 3007–3021, doi:10.5194/acp-6-3007-2006, 2006.

Monahan, E. C. and Muircheartaigh, I. Ó.: Optimal power-law description of oceanic whitecap coverage dependence on wind speed, J. Phys. Oceanogr., 10, 2094–2099, 1980.

Morris, C. E., Sands, D. C., Glaux, C., Samsatly, J., Asaad, S., Moukahel, A. R., Gonçalves, F. L. T. and Bigg, E. K.: Urediospores of rust fungi are ice nucleation active at > −10 °C and harbor ice nucleation active bacteria, Atmos. Chem. Phys., 13, 4223–4233, doi:10.5194/acp-13-4223-2013, 2013.

Morris, C. E., Sands, D. C., Vinatzer, B. A., Glaux, C., Guilbaud, C., Buffière, A., Yan, S., Dominguez, H. and Thompson, B. M.: The life history of the plant pathogen Pseudomonas syringae is linked to the water cycle, ISME J., 2, 321–334, doi: doi:10.1038/ismej.2007.113, 2008.

Murray, B. J., Broadley, S. L., Wilson, T. W., Atkinson, J. D. and Wills, R. H.: Heterogeneous freezing of water droplets containing kaolinite particles, Atmos. Chem. Phys., 11, 4191–4207, doi:10.5194/acp-11-4191-2011, 2011.

Murray, B. J., O'Sullivan, D., Atkinson, J. D. and Webb, M. E.: Ice nucleation by particles immersed in supercooled cloud droplets, Chem. Soc. Rev., 41, 6519–6554, doi:10.1039/c2cs35200a, 2012.

National Data Buoy Center, National Oceanic and Atmospheric Administration, http://www.ndbc.noaa.gov/station_page.php?station=46206 (last accessed: 9 December 2014), 2013.

1356 Niedermeier, D., Hartmann, S., Shaw, R. A., Covert, D., Mentel, T. F., Schneider, J., Poulain, L.,
1357 Reitz, P., Spindler, C., Clauss, T., Kiselev, A., Hallbauer, E., Wex, H., Mildenberger, K. and
1358 Stratmann, F.: Heterogeneous freezing of droplets with immersed mineral dust particles -
1359 measurements and parameterization, Atmos. Chem. Phys., 10, 3601–3614, doi:10.5194/acp-10-
1360 3601-2010, 2010.

1361 O'Dowd, C. D. and de Leeuw, G.: Marine aerosol production: a review of the current
1362 knowledge, Philos. Trans. R. Soc. A, 365, 1753–1774, doi:10.1098/rsta.2007.2043, 2007.

1363 O'Sullivan, D., Murray, B. J., Malkin, T. L., Whale, T. F., Umo, N. S., Atkinson, J. D., Price, H.
1364 C., Baustian, K. J., Browse, J. and Webb, M. E.: Ice nucleation by fertile soil dusts: relative
1365 importance of mineral and biogenic components, Atmos. Chem. Phys., 14, 1853–1867,
1366 doi:10.5194/acp-14-1853-2014, 2014.

1367 O'Sullivan, D., Murray, B. J., Ross, J. F., Whale, T. F., Price, H. C., Atkinson, J. D., Umo, N. S.
1368 and Webb, M. E.: The relevance of nanoscale biological fragments for ice nucleation in clouds,
1369 Sci. Rep., 5, 8082, doi:10.1038/srep08082, 2015.

1370 Pan, Y.-L., Holler, S., Chang, R. K., Hill, S. C., Pinnick, R. G., Niles, S., Bottiger, J. R. and
1371 Bronk, B. V: Real-time detection and characterization of individual flowing airborne biological
1372 particles: fluorescence spectra and elastic scattering measurements, P. Soc. Photo-Opt. Ins.,
1373 3855, 117–125, doi:10.1117/12.371270, 1999.

1374 Parker, L. V, Sullivan, C. W., Forest, T. W. and Ackley, S. F.: Ice nucleation activity of antarctic
1375 marine microorganisms, Antarct. J. US, 20, 126–127, 1985.

1376 Penner, J. E., Chen, Y., Wang, M. and Liu, X.: Possible influence of anthropogenic aerosols on
1377 cirrus clouds and anthropogenic forcing, Atmos. Chem. Phys., 9, 879–896, doi:10.5194/acp-9-
1378 879-2009, 2009.

1379 Petzold, A., Kramer, H. and Schönlinner, M.: Continuous Measurement of Atmospheric Black
1380 Carbon Using a Multi-angle Absorption Photometer, Environ. Sci. Pollut. Res., 4, 78–82, 2002.

1381 Petzold, A., Ogren, J. A., Fiebig, M., Laj, P., Li, S.-M., Baltensperger, U., Holzer-Popp, T.,
1382 Kinne, S., Pappalardo, G., Sugimoto, N., Wehrli, C., Wiedensohler, A. and Zhang, X.-Y.:
1383 Recommendations for reporting "black carbon" measurements, Atmos. Chem. Phys., 13, 8365–
1384 8379, doi:10.5194/acp-13-8365-2013, 2013.

1385 Petzold, A., Schloesser, H., Sheridan, P. J., Arnott, W. P., Ogren, J. A. and Virkkula, A.:
1386 Evaluation of Multiangle Absorption Photometry for Measuring Aerosol Light Absorption,
1387 Aerosol Sci. Technol., 39, 40–51, doi:10.1080/027868290901945, 2005.

1388 Petzold, A. and Schönlinner, M.: Multi-angle absorption photometry - a new method for the
1389 measurement of aerosol light absorption and atmospheric black carbon, J. Aerosol Sci., 35, 421–
1390 441, doi:10.1016/j.jaerosci.2003.09.005, 2004.

1391 Phillips, V. T. J., Andronache, C., Christner, B., Morris, C. E., Sands, D. C., Bansemer, A.,
1392 Lauer, A., McNaughton, C. and Seman, C.: Potential impacts from biological aerosols on
1393 ensembles of continental clouds simulated numerically, Biogeosciences, 6, 987–1014,
1394 doi:10.5194/bg-6-987-2009, 2009.

1395 Phinney, L., Leaitch, W. R., Lohmann, U., Boudries, H., Worsnop, D. R., Jayne, J. T., Toom-
1396 Sauntry, D., Wadleigh, M., Sharma, S. and Shantz, N.: Characterization of the aerosol over the

sub-arctic north east Pacific Ocean, Deep-Sea Res. Pt. II, 53, 2410–2433, doi:10.1016/j.dsr2.2006.05.044, 2006.

Pöhlker, C., Huffman, J. A. and Pöschl, U.: Autofluorescence of atmospheric bioaerosols - fluorescent biomolecules and potential interferences, Atmos. Meas. Tech., 5, 37–71, doi:10.5194/amt-5-37-2012, 2012.

Pouleur, S., Richard, C., Martin, J.-G. and Antoun, H.: Ice Nucleation Activity in *Fusarium acuminatum* and *Fusarium avenaceum*, Appl. Environ. Microbiol., 58, 2960–2964, 1992.

Prather, K. A., Bertram, T. H., Grassian, V. H., Deane, G. B., Stokes, M. D., DeMott, P. J., Aluwihare, L. I., Palenik, B. P., Azam, F., Seinfeld, J. H., Moffet, R. C., Molina, M. J., Cappa, C. D., Geiger, F. M., Roberts, G. C., Russell, L. M., Ault, A. P., Baltrusaitis, J., Collins, D. B., Corrigan, C. E., Cuadra-Rodriguez, L. A., Ebben, C. J., Forestieri, S. D., Guasco, T. L., Hersey, S. P., Kim, M. J., Lambert, W. F., Modini, R. L., Mui, W., Pedler, B. E., Ruppel, M. J., Ryder, O. S., Schoepp, N. G., Sullivan, R. C. and Zhao, D.: Bringing the ocean into the laboratory to probe the chemical complexity of sea spray aerosol, P. Natl. Acad. Sci. USA, 110, 7550–7555, doi:10.1073/pnas.1300262110, 2013.

Pratt, K. A., DeMott, P. J., French, J. R., Wang, Z., Westphal, D. L., Heymsfield, A. J., Twohy, C. H., Prenni, A. J. and Prather, K. A.: In situ detection of biological particles in cloud ice-crystals, Nat. Geosci., 2, 398–401, doi:10.1038/ngeo521, 2009.

Prenni, A. J., Petters, M. D., Kreidenweis, S. M., Heald, C. L., Martin, S. T., Artaxo, P., Garland, R. M., Wollny, A. G. and Pöschl, U.: Relative roles of biogenic emissions and Saharan dust as ice nuclei in the Amazon basin, Nat. Geosci., 2, 402–405, doi:10.1038/ngeo517, 2009.

Prenni, A. J., Tobo, Y., Garcia, E., DeMott, P. J., Huffman, J. A., McCluskey, C. S., Kreidenweis, S. M., Prenni, J. E., Pöhlker, C. and Pöschl, U.: The impact of rain on ice nuclei populations at a forested site in Colorado, Geophys. Res. Lett., 40, 227–231, doi:10.1029/2012GL053953, 2013.

Pummer, B. G., Bauer, H., Bernardi, J., Bleicher, S. and Grothe, H.: Suspendable macromolecules are responsible for ice nucleation activity of birch and conifer pollen, Atmos. Chem. Phys., 12, 2541–2550, doi:10.5194/acp-12-2541-2012, 2012.

Ribalet, F., Marchetti, A., Hubbard, K. A., Brown, K., Durkin, C. A., Morales, R., Robert, M., Swalwell, J. E., Tortell, P. D. and Armbrust, E. V.: Unveiling a phytoplankton hotspot at a narrow boundary between coastal and offshore waters, P. Natl. Acad. Sci. USA, 107, 16571–16576, doi:10.1073/pnas.1005638107, 2010.

Richard, C., Martin, J.-G. and Pouleur, S.: Ice nucleation activity identified in some phytopathogenic *Fusarium* species, Phytoprotection, 77, 83–92, doi:10.7202/706104ar, 1996.

Richardson, M. S., DeMott, P. J., Kreidenweis, S. M., Cziczo, D. J., Dunlea, E. J., Jimenez, J. L., Thomson, D. S., Ashbaugh, L. L., Borys, R. D., Westphal, D. L., Casuccio, G. S. and Lersch, T. L.: Measurements of heterogeneous ice nuclei in the western United States in springtime and their relation to aerosol characteristics, J. Geophys. Res., 112, D02209, doi:10.1029/2006JD007500, 2007.

Rogers, D. C., DeMott, P. J., Kreidenweis, S. M. and Chen, Y.: Measurements of ice nucleating aerosols during SUCCESS, Geophys. Res. Lett., 25, 1383–1386, doi:10.1029/97GL03478, 1998.

1438 Saltzman, E. S., Savoie, D. L., Prospero, J. M. and Zika, R. G.: Methanesulfonic acid and non-
1439 sea-salt sulfate in Pacific air: Regional and seasonal variations, J. Atmos. Chem., 4, 227–240,
1440 doi:10.1007/BF00052002, 1986.

1441 Savoie, D. L., Prospero, J. M., Arimoto, R. and Duce, R. A.: Non-sea-salt sulfate and
1442 methanesulfonate at American Samoa, J. Geophys. Res., 99, 3587–3596,
1443 doi:10.1029/93JD03337, 1994.

1444 Schnell, R. C.: Ice nuclei produced by laboratory cultured marine phytoplankton, Geophys. Res.
1445 Lett., 2, 500–502, doi:10.1029/GL002i011p00500, 1975.

1446 Schnell, R. C.: Ice Nuclei in Seawater, Fog Water and Marine Air off the Coast of Nova Scotia:
1447 Summer 1975, J. Atmos. Sci., 34, 1299–1305, 1977.

1448 Schnell, R. C. and Vali, G.: Freezing nuclei in marine waters, Tellus, 27, 321–323,
1449 doi:10.1111/j.2153-3490.1975.tb01682.x, 1975.

1450 Schroder, J. C., Hanna, S. J., Modini, R. L., Corrigan, A. L., Kreidenweis, S. M., Macdonald, A.
1451 M., Noone, K. J., Russell, L. M., Leaitch, W. R. and Bertram, A. K.: Size-resolved observations
1452 of refractory black carbon particles in cloud droplets at a marine boundary layer site, Atmos.
1453 Chem. Phys., 15, 1367–1383, doi:10.5194/acp-15-1367-2015, 2015.

1454 Schwarz, J. P., Gao, R. S., Perring, A. E., Spackman, J. R. and Fahey, D. W.: Black carbon
1455 aerosol size in snow, Sci. Rep., 3, 1356, doi:10.1038/srep01356, 2013.

1456 Schwarz, J. P., Gao, R. S., Spackman, J. R., Watts, L. A., Thomson, D. S., Fahey, D. W.,
1457 Ryerson, T. B., Peischl, J., Holloway, J. S., Trainer, M., Frost, G. J., Baynard, T., Lack, D. A., de
1458 Gouw, J. A., Warneke, C. and Del Negro, L. A.: Measurement of the mixing state, mass, and
1459 optical size of individual black carbon particles in urban and biomass burning emissions,
1460 Geophys. Res. Lett., 35, L13810, doi:10.1029/2008GL033968, 2008.

1461 Sesartic, A., Lohmann, U. and Storelvmo, T.: Modelling the impact of fungal spore ice nuclei on
1462 clouds and precipitation, Environ. Res. Lett., 8, 014029, doi:10.1088/1748-9326/8/1/014029,
1463 2013.

1464 Sivaprakasam, V., Huston, A., Scotto, C. and Eversole, J.: Multiple UV wavelength excitation
1465 and fluorescence of bioaerosols, Opt. Express, 12, 4457–4466, doi:10.1364/OPEX.12.004457,
1466 2004.

1467 Sorooshian, A., Padró, L. T., Nenes, A., Feingold, G., McComiskey, A., Hersey, S. P., Gates, H.,
1468 Jonsson, H. H., Miller, S. D., Stephens, G. L., Flagan, R. C. and Seinfeld, J. H.: On the link
1469 between ocean biota emissions, aerosol, and maritime clouds: Airborne, ground, and satellite
1470 measurements off the coast of California, Global Biogeochem. Cycles, 23, GB4007,
1471 doi:10.1029/2009GB003464, 2009.

1472 Spracklen, D. V and Heald, C. L.: The contribution of fungal spores and bacteria to regional and
1473 global aerosol number and ice nucleation immersion freezing rates, Atmos. Chem. Phys., 14,
1474 9051–9059, doi:10.5194/acp-14-9051-2014, 2014.

1475 Statistics Canada, Catalogue no. 98-316-XWE, available at: http://www12.statcan.gc.ca/census-
1476 recensement/2011/dp-pd/prof/index.cfm?Lang=E (last access: 4 November 2014), Ottawa, 2012.

1477 Storelvmo, T., Hoose, C. and Eriksson, P.: Global modeling of mixed-phase clouds: The albedo
1478 and lifetime effects of aerosols, J. Geophys. Res., 116, D05207, doi:10.1029/2010JD014724,
1479 2011.

1480 Sun, J., Ariya, P. A., Leighton, H. G. and Yau, M. K.: Modeling Study of Ice Formation in
1481 Warm-Based Precipitating Shallow Cumulus Clouds, J. Atmos. Sci., 69, 3315–3335,
1482 doi:10.1175/JAS-D-11-0344.1, 2012.

1483 Szyrmer, W. and Zawadzki, I.: Biogenic and anthropogenic sources of ice-forming nuclei: A
1484 review, B. Am. Meteorol. Soc., 78, 209–228, 1997.

1485 Tobo, Y., DeMott, P. J., Hill, T. C. J., Prenni, A. J., Swoboda-Colberg, N. G., Franc, G. D. and
1486 Kreidenweis, S. M.: Organic matter matters for ice nuclei of agricultural soil origin, Atmos.
1487 Chem. Phys., 14, 8521–8531, doi:10.5194/acp-14-8521-2014, 2014.

1488 Tobo, Y., Prenni, A. J., DeMott, P. J., Huffman, J. A., McCluskey, C. S., Tian, G., Pöhlker, C.,
1489 Pöschl, U. and Kreidenweis, S. M.: Biological aerosol particles as a key determinant of ice nuclei
1490 populations in a forest ecosystem, J. Geophys. Res.-Atmos., 118, 10100–10110,
1491 doi:10.1002/jgrd.50801, 2013.

1492 Tsumuki, H., Konno, H., Maeda, T. and Okamoto, Y.: An ice-nucleating active fungus isolated
1493 from the gut of the rice stem borer, *Chilo suppressalis* Walker (Lepidoptera: Pyralidae), J. Insect
1494 Physiol., 38, 119–125, doi:10.1016/0022-1910(92)90040-K, 1992.

1495 Twohy, C. H., DeMott, P. J., Pratt, K. A., Subramanian, R., Kok, G. L., Murphy, S. M., Lersch,
1496 T., Heymsfield, A. J., Wang, Z., Prather, K. A. and Seinfeld, J. H.: Relationships of Biomass-
1497 Burning Aerosols to Ice in Orographic Wave Clouds, J. Atmos. Sci., 67, 2437–2450,
1498 doi:10.1175/2010JAS3310.1, 2010.

1499 United States Environmental Protection Agency, Air Emission Sources,
1500 http://www.epa.gov/air/emissions/index.htm (last access: 7 April 2015), 2014.

1501 Vali, G.: Quantitative Evaluation of Experimental Results on the Heterogeneous Freezing
1502 Nucleation of Supercooled Liquids, J. Atmos. Sci., 28, 402–409, 1971.

1503 Vali, G.: Nucleation Terminology, J. Aerosol Sci., 16, 575–576, doi:10.1016/0021-
1504 8502(85)90009-6, 1985.

1505 Vali, G., DeMott, P. J., Möhler, O. and Whale, T. F.: Technical Note: A proposal for ice
1506 nucleation terminology, Atmos. Chem. Phys., 15, 10263–10270, doi:10.5194/acp-15-10263-
1507 2015, 2015.

1508 von Blohn, N., Mitra, S. K., Diehl, K. and Borrmann, S.: The ice nucleating ability of pollen:
1509 Part III. New laboratory studies in immersion and contact freezing modes including more pollen
1510 types, Atmos. Res., 78, 182–189, doi:10.1016/j.atmosres.2005.03.008, 2005.

1511 Webster, J. and Weber, R. W. S.: Introduction to Fungi, Third Edition, Cambridge University
1512 Press, New York, NY, USA, 2007.

1513 Welti, A., Lüönd, F., Kanji, Z. A., Stetzer, O. and Lohmann, U.: Time dependence of immersion
1514 freezing: an experimental study on size selected kaolinite particles, Atmos. Chem. Phys., 12,
1515 9893–9907, doi:10.5194/acp-12-9893-2012, 2012.

Wheeler, M. J. and Bertram, A. K.: Deposition nucleation on mineral dust particles: a case against classical nucleation theory with the assumption of a single contact angle, Atmos. Chem. Phys., 12, 1189–1201, doi:10.5194/acp-12-1189-2012, 2012.

Wheeler, M. J., Mason, R. H., Steunenberg, K., Wagstaff, M., Chou, C. and Bertram, A. K.: Immersion Freezing of Supermicron Mineral Dust Particles: Freezing Results, Testing Different Schemes for Describing Ice Nucleation, and Ice Nucleation Active Site Densities, J. Phys. Chem. A, 119, 4358–4372, doi:10.1021/jp507875q, 2015.

Whitney, F. A., Crawford, W. R. and Harrison, P. J.: Physical processes that enhance nutrient transport and primary productivity in the coastal and open ocean of the subarctic NE Pacific, Deep Sea Res. Part II Top. Stud. Oceanogr., 52, 681–706, doi:10.1016/j.dsr2.2004.12.023, 2005.

Wilson, T. W., Ladino, L. A., Alpert, P. A., Breckels, M. N., Brooks, I. M., Browse, J., Burrows, S. M., Carslaw, K. S., Huffman, J. A., Judd, C., Kilthau, W. P., Mason, R. H., McFiggans, G., Miller, L. A., Nájera, J. J., Polishchuk, E., Rae, S., Schiller, C. L., Si, M., Vergara Temprado, J., Whale, T. F., Wong, J. P. S., Wurl, O., Yakobi-Hancock, J. D., Abbatt, J. P. D., Aller, J. Y., Bertram, A. K., Knopf, D. A. and Murray, B. J.: A marine biogenic source of atmospheric ice nucleating particles, Nature, 525, 234–238, doi:10.1038/nature14986, 2015.

Wright, T. P. and Petters, M. D.: The role of time in heterogeneous freezing nucleation, J. Geophys. Res.-Atmos., 118, 3731–3743, doi:10.1002/jgrd.50365, 2013.

Wright, T. P., Petters, M. D., Hader, J. D., Morton, T. and Holder, A. L.: Minimal cooling rate dependence of ice nuclei activity in the immersion mode, J. Geophys. Res.-Atmos., 118, 10535–10543, doi:10.1002/jgrd.50810, 2013.

Yakobi-Hancock, J. D., Ladino, L. A. and Abbatt, J. P. D.: Feldspar minerals as efficient deposition ice nuclei, Atmos. Chem. Phys., 13, 11175–11185, doi:10.5194/acp-13-11175-2013, 2013.

Yakobi-Hancock, J. D., Ladino, L. A., Bertram, A. K., Huffman, J. A., Jones, K., Leaitch, W. R., Mason, R. H., Schiller, C. L., Toom-Sauntry, D., Wong, J. P. S. and Abbatt, J. P. D.: CCN activity of size-selected aerosol at a Pacific coastal location, Atmos. Chem. Phys., 14, 12307–12317, doi:10.5194/acp-14-12307-2014, 2014.

Yang, M., Howell, S. G., Zhuang, J. and Huebert, B. J.: Attribution of aerosol light absorption to black carbon, brown carbon, and dust in China - interpretations of atmospheric measurements during EAST-AIRE, Atmos. Chem. Phys., 9, 2035–2050, doi:10.5194/acp-9-2035-2009, 2009.

Yun, Y. and Penner, J. E.: An evaluation of the potential radiative forcing and climatic impact of marine organic aerosols as heterogeneous ice nuclei, Geophys. Res. Lett., 40, 4121–4126, doi:10.1002/grl.50794, 2013.

Zimmermann, F., Weinbruch, S., Schütz, L., Hofmann, H., Ebert, M., Kandler, K. and Worringen, A.: Ice nucleation properties of the most abundant mineral dust phases, J. Geophys. Res., 113, D23204, doi:10.1029/2008JD010655, 2008.

Table 1. Correlation coefficients (R) for linear regression analyses of INPs versus fluorescent bioparticles, total aerosol particles, eBC, sodium, MSA, and wind speed[a]. Correlations with statistical significance ($P < 0.05$) are shown in bold.

	Relation to the INP number concentration											
	-15 °C			-20 °C			-25 °C			-30 °C		
Measurement	R	P[b]	n[c]	R	P	n	R	P	n	R	P	n
Fluorescent bioparticles [0.5–10 µm]	**0.74**	< 0.01	28	**0.77**	< 0.01	28	**0.83**	< 0.01	28	**0.66**	< 0.01	23
Total particles [0.5–10 µm]	**0.33**	0.04	28	**0.36**	0.03	28	**0.49**	< 0.01	28	**0.66**	< 0.01	23
eBC	**0.47**	< 0.01	34	**0.59**	< 0.01	34	**0.60**	< 0.01	34	0.25	0.11	27
Sodium	-0.35	0.25	6	0.13	0.40	6	0.32	0.27	6	0.82	0.20	3
MSA	0.17	0.38	6	0.51	0.15	6	0.27	0.30	6	0.00	0.50	3
(Wind speed)$^{3.41}$ [lighthouse]	0.05	0.39	34	0.01	0.48	34	0.15	0.19	34	**0.48**	< 0.01	27
(Wind speed)$^{3.41}$ [buoy]	0.04	0.40	34	0.04	0.40	34	0.19	0.14	34	**0.55**	< 0.01	27

[a]Using the power law dependence of whitecap coverage on wind speed found by Monahan and Muircheartaigh (1980), wind speed was raised to the power of 3.41.
[b]The P value is a conditional probability that is the probability of obtaining an R value equal to or greater than the given R value if there is no correlation between INPs and the given parameter.
[c]n represents the number of data points used in determining the correlation.

Ryan Mason 9/21/2015 1:34 PM
Formatted Table

Table 2. Correlation coefficients (R) for linear regression analyses of INPs versus fluorescent bioparticles, total aerosol particles, eBC, and wind speed[a] within each category of air mass. Correlations with statistical significance ($P < 0.05$) are shown in bold.

		Relation to the INP number concentration											
		-15 °C			-20 °C			-25 °C			-30 °C		
Air Mass	Measurement	R	P[b]	n[c]	R	P	n	R	P	n	R	P	n
Coastal NW	Fluorescent bioparticles [0.5–10 µm]	**0.94**	<0.01	9	**0.94**	<0.01	9	**0.96**	<0.01	9	0.65	0.08	6
	Total particles [0.5–10 µm]	**0.85**	<0.01	9	**0.70**	0.02	9	**0.71**	0.02	9	0.67	0.07	6
	eBC	**0.71**	<0.01	11	**0.80**	<0.01	11	**0.84**	<0.01	11	0.53	0.11	7
	(Wind speed)$^{3.41}$ [lighthouse]	-0.38	0.12	11	-0.39	0.12	11	-0.22	0.26	11	0.26	0.29	7
	(Wind speed)$^{3.41}$ [buoy]	-0.03	0.47	11	0.00	0.49	11	0.00	0.50	11	-0.02	0.48	7
Coastal SE	Fluorescent bioparticles [0.5–10 µm]	-0.07	0.48	3	-0.53	0.32	3	-0.85	0.17	3	NA[d]		
	Total particles [0.5–10 µm]	-0.17	0.45	3	-0.61	0.29	3	-0.90	0.14	3	NA		
	eBC	0.07	0.46	5	0.28	0.32	5	0.67	0.11	5	0.96	0.09	3
	(Wind speed)$^{3.41}$ [lighthouse]	-0.34	0.29	5	-0.27	0.33	5	-0.14	0.41	5	0.21	0.43	3
	(Wind speed)$^{3.41}$ [buoy]	-0.52	0.18	5	-0.37	0.27	5	-0.12	0.43	5	0.93	0.12	3
Pacific Ocean	Fluorescent bioparticles [0.5–10 µm]	**0.80**	<0.01	12	**0.74**	<0.01	12	**0.64**	0.01	12	0.23	0.24	12
	Total particles [0.5–10 µm]	0.13	0.34	12	0.30	0.17	12	0.21	0.25	12	0.25	0.22	12
	eBC	0.24	0.21	14	0.37	0.10	14	0.26	0.19	14	0.06	0.42	13
	(Wind speed)$^{3.41}$ [lighthouse]	-0.10	0.37	14	-0.26	0.18	14	-0.26	0.19	14	-0.21	0.25	13
	(Wind speed)$^{3.41}$ [buoy]	-0.18	0.27	14	-0.38	0.09	14	**-0.48**	0.04	14	-0.22	0.23	13
Free troposphere	Fluorescent bioparticles [0.5–10 µm]	**0.97**	0.02	4	**0.99**	<0.01	4	**0.99**	<0.01	4	**1.00**	<0.01	4
	Total particles [0.5–10 µm]	0.86	0.07	4	**0.98**	0.01	4	**0.99**	<0.01	4	**0.98**	0.01	4
	eBC	**0.99**	<0.01	4	0.89	0.05	4	0.88	0.06	4	0.89	0.06	4
	(Wind speed)$^{3.41}$ [lighthouse]	-0.89	0.05	4	-0.70	0.15	4	-0.67	0.17	4	-0.68	0.16	4
	(Wind speed)$^{3.41}$ [buoy]	0.62	0.19	4	0.39	0.31	4	0.38	0.31	4	0.42	0.29	4

[a]Using the power law dependence of whitecap coverage on wind speed found by Monahan and Muircheartaigh (1980), wind speed was raised to the power of 3.41.
[b]The P value is a conditional probability that is the probability of obtaining an R value equal to or greater than the given R value if there is no correlation between INPs and the given parameter.
[c]n represents the number of data points used in determining the correlation.
[d]NA = not available due to insufficient data.

Ryan Mason 9/21/2015 2:04 PM
Formatted Table

Ryan Mason 9/21/2015 2:04 PM
Formatted Table

Ryan Mason 9/21/2015 2:06 PM
Deleted: (Wind speed)$^{3.41}$

Ryan Mason 9/21/2015 2:04 PM
Formatted Table

Ryan Mason 9/21/2015 2:06 PM
Deleted: (Wind speed)$^{3.41}$

Ryan Mason 9/21/2015 2:11 PM
Formatted: Font:Not Italic

Ryan Mason 9/21/2015 2:03 PM
Formatted Table

Ryan Mason 9/21/2015 2:06 PM
Deleted: (Wind speed)$^{3.41}$

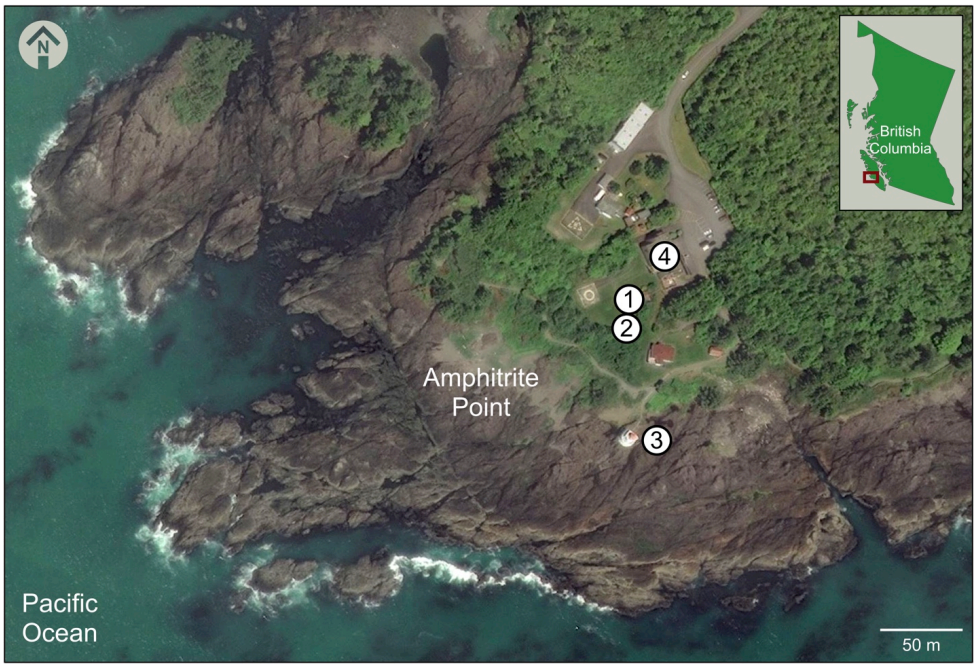

Figure 1. A satellite image of the sampling site: (1) location of the MOUDIs and the WIBS-4A; (2) location of the MAAP; (3) Amphitrite Lighthouse where most meteorological data was collected; and (4) a station of the Canadian Coast Guard with supporting infrastructure. The image was modified from Bing Maps, 2014 (http://www.bing.com/maps/). Inset: the location of the sampling site in British Columbia, Canada.

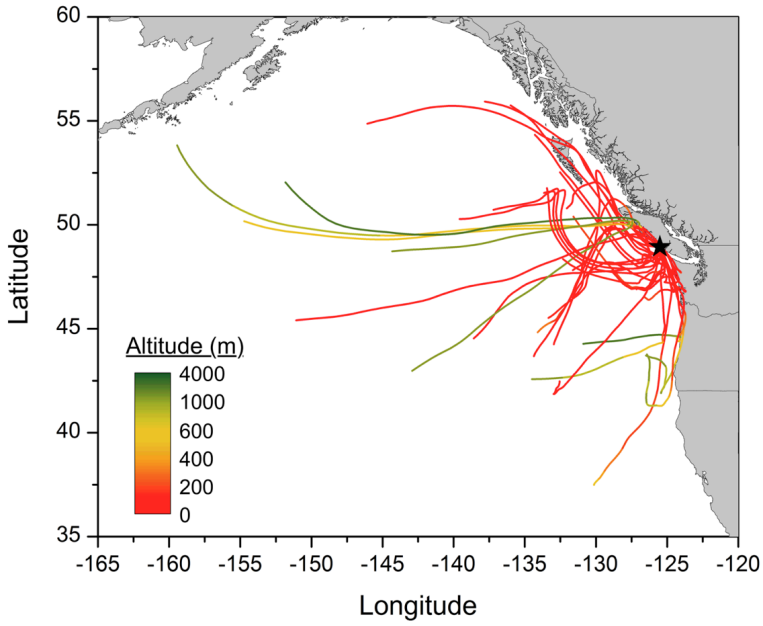

Figure 2. Seventy-two hour HYSPLIT4 back trajectories of the air masses analyzed at the coastal site (black star) during INP sampling periods. Each back trajectory was initiated from a height of 5.5 m agl and at the midpoint of the sampling period.

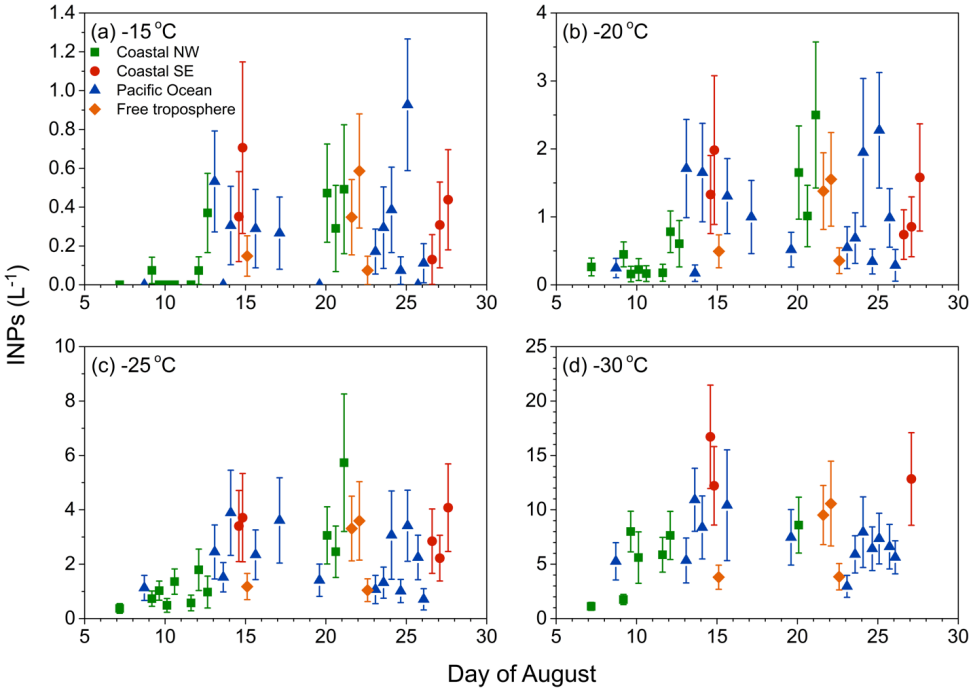

Figure 3. INP number concentrations as a function of date determined at ice-activation temperatures of (a) -15 °C, (b) -20 °C, (c) -25 °C, and (d) -30 °C. The symbols are color coded by air mass category (see Sect. 2.8 for details). Fewer data points are available at -30 °C as INP number concentrations can only be determined to the temperature where all droplets are frozen and Eq. (1) becomes undefined.

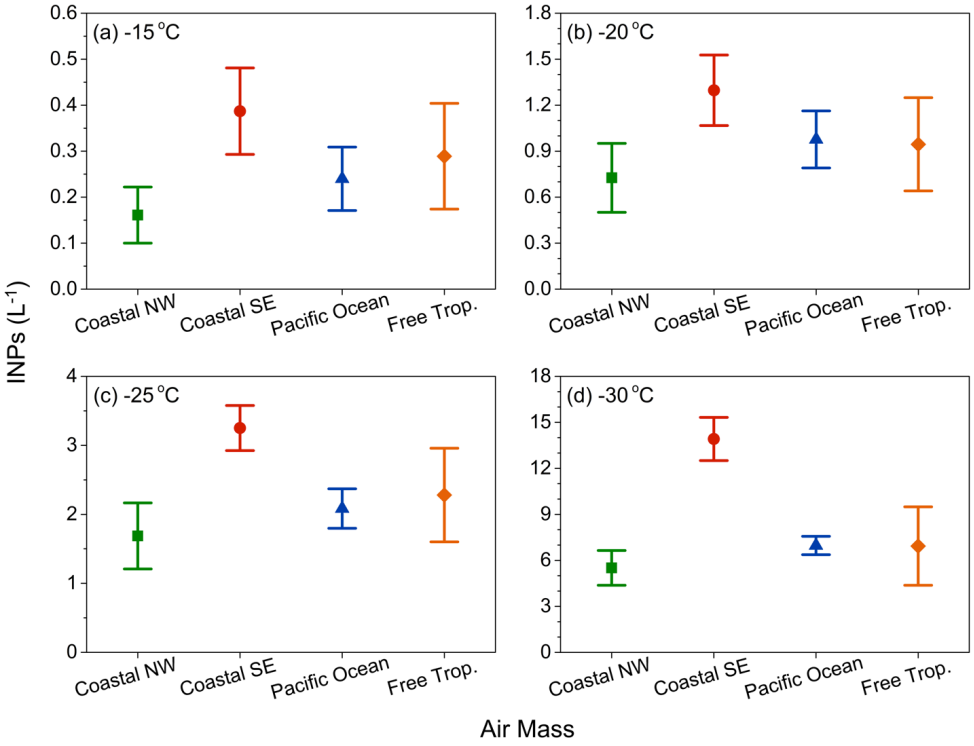

Figure 4. Mean INP number concentrations found in each of the four categories of air masses sampled at (a) -15 °C, (b) -20 °C, (c) -25 °C, and (d) -30 °C. The scheme for air mass classification is given in Sect. 2.8. Uncertainties are given as the standard error of the mean.

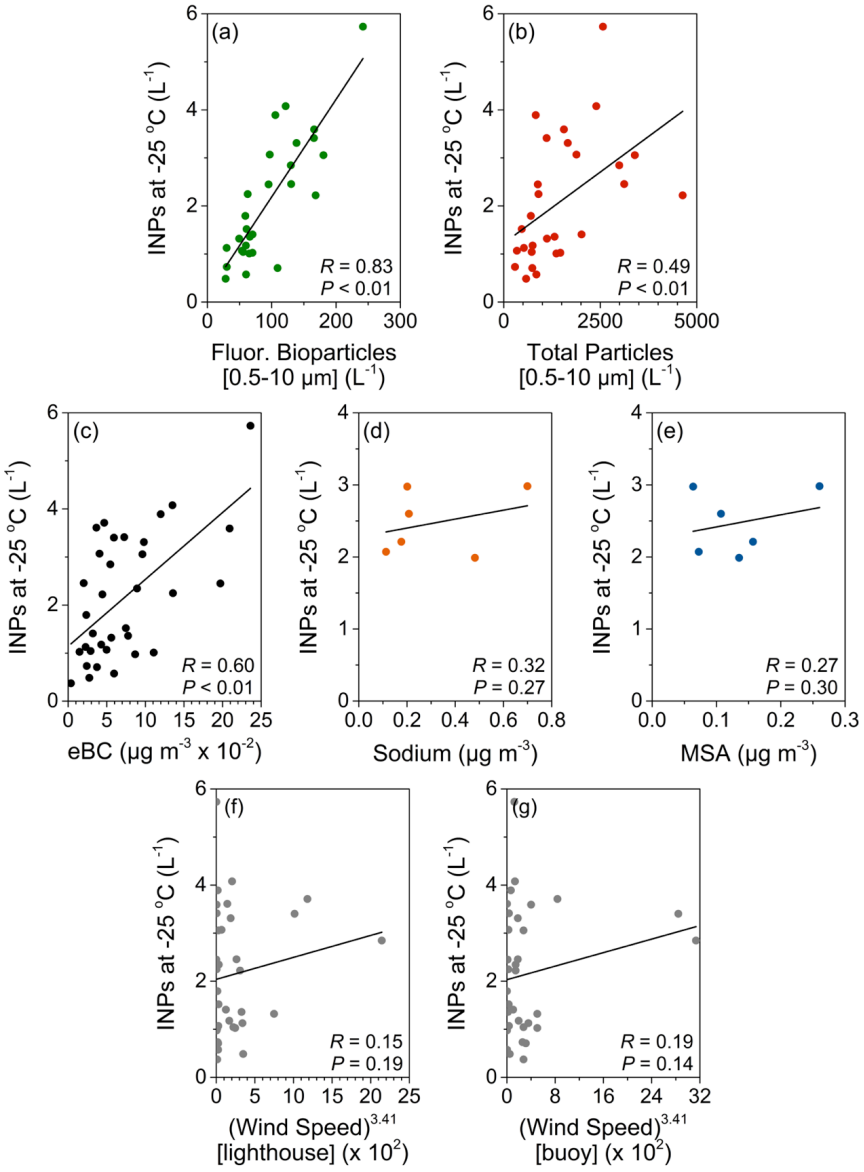

Figure 5. Number concentrations of INPs active at -25 °C plotted against concentrations of (a) fluorescent bioparticles 0.5–10 µm, (b) total particles 0.5–10 µm, (c) eBC, (d) sodium, (e) MSA, and (f–g) (wind speed)$^{3.41}$ based on the power law function of Monahan and Muircheartaigh (1980) where wind speed was in units of m s^{-1}. Linear fits are shown with corresponding correlation coefficients (R) and probability values (P).

Ryan Mason 10/4/2015 11:00 AM
Comment [3]: Modified to include buoy data.

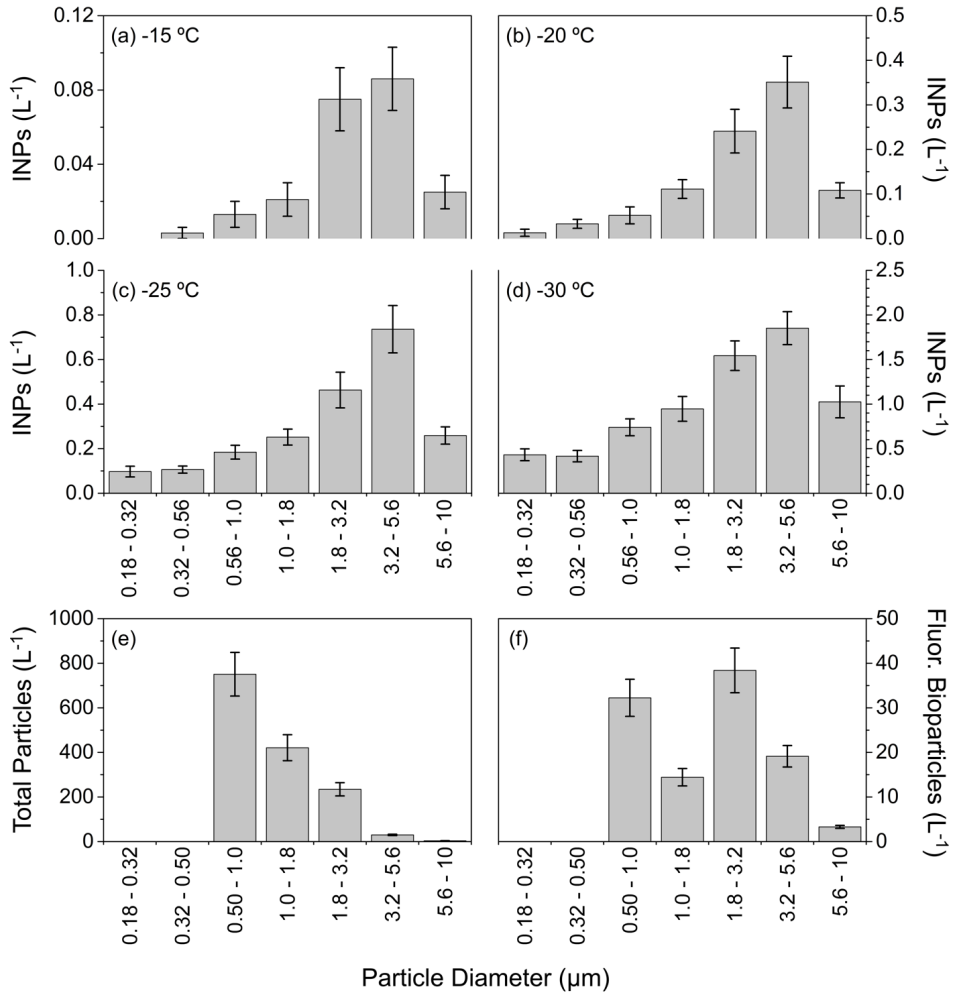

Figure 6. Mean number concentrations as a function of size for INPs active at (a) -15 °C, (b) -20 °C, (c) -25 °C, and (d) -30 °C, total particles (e) and fluorescent bioparticles (f) using only samples where both the MOUDI-DFT and WIBS-4A were operating. Uncertainties are given as the standard error of the mean. As INP number concentrations can only be determined at temperatures less than the temperature where all droplets are frozen and Eq. (1) becomes undefined, fewer samples are represented at -30 °C. Number concentrations below 0.5 µm were not measured by the WIBS-4A for panels (e) and (f) but plot axes are consistent for easier comparison of the size distributions.

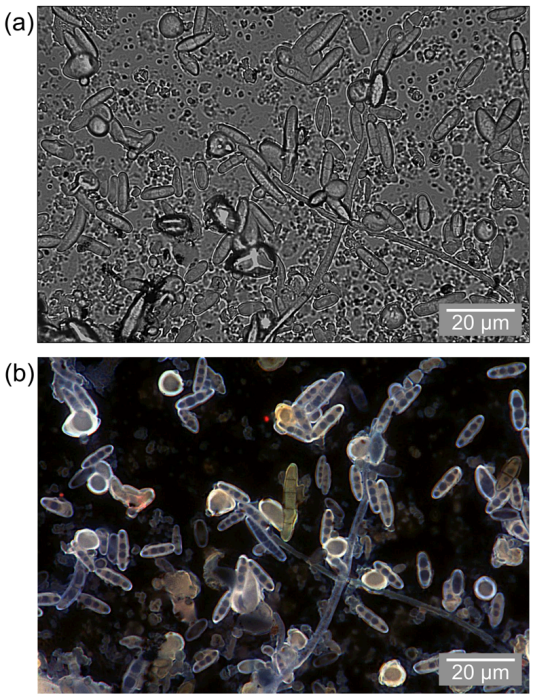

Figure 7. Fluorescence microscopy images of an aerosol sample collected on August 11, 2013: (a) bright-field image; (b) an overlay of red, green, and blue fluorescence channels. A blue coloration is characteristic of biological material (Pöhlker et al., 2012).

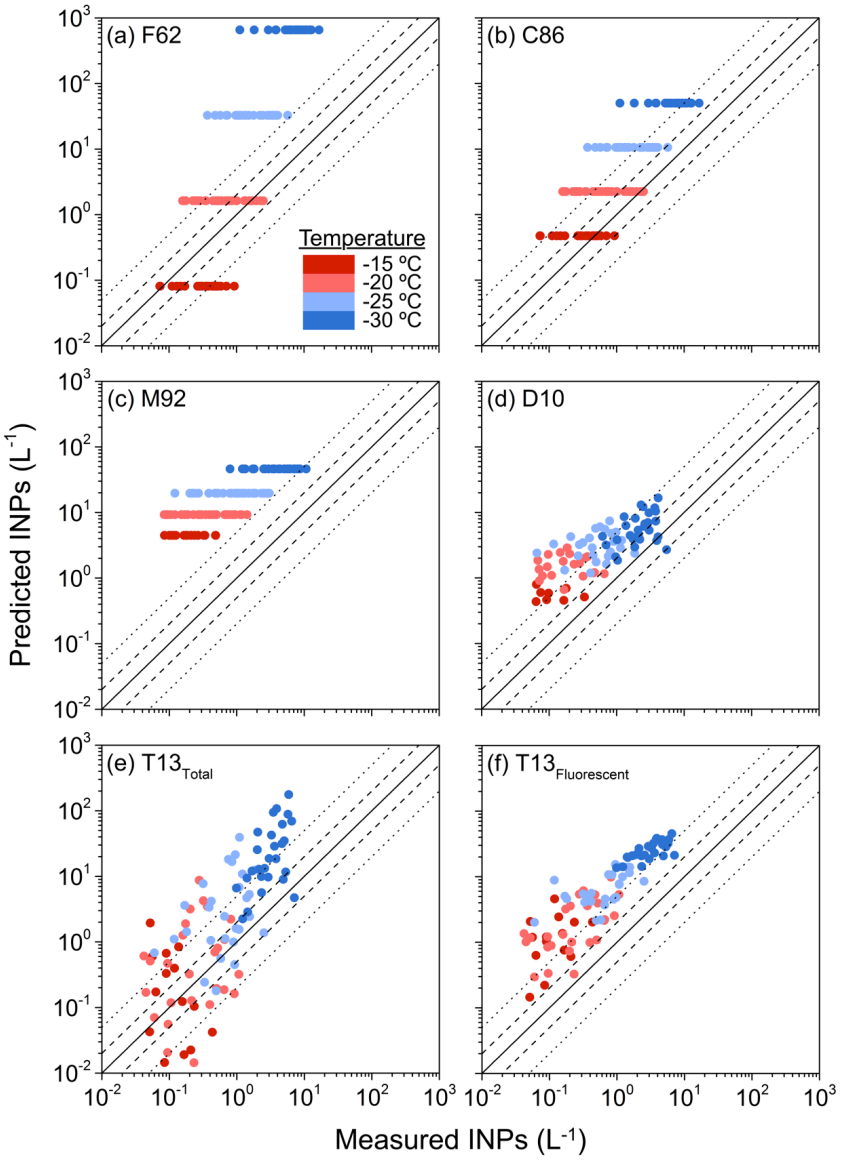

Figure 8. Predicted versus measured INP number concentrations based on the parameterizations of (a) Fletcher (1962); (b) Cooper (1986); (c) Meyers et al. (1992); (d) DeMott et al. (2010); and (e–f) Tobo et al. (2013). Details on these parameterizations are given in the Supplement. Data color represents ice nucleation temperatures. This figure uses the format of Fig. 9 in Tobo et al. (2013).

Do this plot for: sum of fluor. particles
AND/OR
: separately for each size range
e.g.
size 1 size 2 size 3